Vascular Tumors

16

Mariem Ben Haj Amor, Caroline Degrugillier-Chopinet, Alexandre Bridoux, François Pontana, Luc Ceugnart, and Anne Cotten

Contents

M.B.H. Amor, MD • L. Ceugnart, MD
Service de Radiologie, Centre Oscar Lambret, 3, Rue Fréderic Combemale, 59000 Lille, France
e-mail: m-benhajamor@o-lambret.fr; l-ceugnart@o-lambret.fr

C. Degrugillier-Chopinet, MD
Service de Neuroradiologie, CHRU de Lille, 59037 Lille, France
e-mail: caroline.chopinet@chru-lille.fr

A. Bridoux, MD • A. Cotten, MD, PhD (✉)
Service de Radiologie et Imagerie Musculosquelettique, Centre de Consultations et d'Imagerie de l'Appareil Locomoteur, CHRU de Lille, 59037 Lille, France
e-mail: alexandre.bridoux@hotmail.fr; anne.cotten@chru-lille.fr

F. Pontana, MD, PhD
Service de Radiologie et d'Imagerie Cardiaque et Vasculaire, CHRU de Lille, 59037 Lille, France
e-mail: francois.pontana@chru-lille.fr

16.1 Introduction

Vascular soft tissue lesions represent a wide and heterogeneous spectrum of lesions. Most of the lesions are recognized on clinical history and physical examination. When imaging is requested, it should be targeted to address specific issues such as planning therapeutic management by a multidisciplinary team [1].

Ultrasound (US) coupled with color Doppler US is traditionally considered the imaging modality of choice for the initial assessment and characterization of a lesion of presumed vascular origin [2]. Magnetic resonance imaging (MRI) in combination with dynamic magnetic resonance

F.M. Vanhoenacker et al. (eds.), *Imaging of Soft Tissue Tumors*, DOI 10.1007/978-3-319-46679-8_16

(MR) angiography is the most valuable modality for the classification of vascular anomalies [3]. Its role in evaluating the extent and relationship of the lesion to the adjacent structures is important, particularly for therapy planning. The aim of this chapter is to review the spectrum of vascular and lymphatic lesions of the musculoskeletal system.

16.2 Classification

The use of different terminologies in the literature for vascular lesions has led to considerable confusion [4]. For example, the term hemangioma has been applied to many vascular lesions of differing origins and clinical behaviors. Because the treatment strategy depends on the type of vascular anomaly, the correct diagnosis and classification are critical.

Several classification systems have been described but the two main classifications are:

- The classification system defined by the World Health Organization's (WHO) Committee for the Classification of Soft Tissue Tumors [5]
- The classification system defined by the International Society for the Study of Vascular Anomalies (ISSVA) [6]

These two classifications show differences in terminology for benign lesions, but they are in agreement for intermediate and malignant tumors.

16.2.1 WHO Classification

The WHO classification is based on the pathological aspects of the soft tissue tumors (Table 16.1 and Chap. 11) [5]. The term of hemangioma is defined as "a benign nonreactive lesion with an increase in the number of normal- or abnormal-appearing vessels" [7]. Subdivisions are based on the predominant type of vascular channel. No distinction is made between benign vascular tumors and vascular malformations.

Table 16.1 Histological classification of vascular tumors, WHO 2013 [5]

Benign vascular tumors
Hemangiomas of subcutaneous/deep soft tissue
Capillary
Cavernous
Arteriovenous
Venous
Intramuscular
Synovial
Epithelioid hemangioma
Angiomatosis
Lymphangioma
Vascular tumors of intermediate malignancy (locally aggressive)
Kaposiform hemangioendothelioma
Vascular tumors of intermediate malignancy (rarely metastasizing)
Retiform hemangioendothelioma
Papillary intralymphatic angioendothelioma
Composite hemangioendothelioma
Kaposi's sarcoma
Malignant vascular tumors
Epithelioid hemangioendothelioma
Angiosarcoma

16.2.2 ISSVA Classification

In 1982, Mulliken and Glowacki [8] proposed a useful classification for vascular anomalies, which was then adopted by the International Society for the Study of Vascular Anomalies (ISSVA) in 1996 and updated in 2014 [6]. This classification is based on the cellular turnover, histologic features, natural history, and physical findings of the vascular anomalies [8]. Lesions are divided into tumors (neoplastic growth of vascular endothelial cells) and vascular malformations (vascular structural anomalies with normal endothelial turnover) [6, 8, 9] (Table 16.2).

The use of this classification system has been strongly recommended in recent years because of its effectiveness and usefulness for determining the appropriate treatment in patients with vascular lesions, particularly in pediatric patients where vascular lesions represent the most common cause of soft tissue lesion [10].

Table 16.2 ISSVA classification of vascular tumors and malformations

Tumors
Benign
Infantile hemangioma
Congenital hemangioma (RICH, NICH, PICH)[a]
Others: tufted angioma, spindle cell hemangioma, epithelioid hemangioma, pyogenic granuloma
Locally aggressive or borderline
Kaposiform hemangioendothelioma, retiform hemangioendothelioma
Papillary intralymphatic angioendothelioma (PILA), Dabska tumor
Composite hemangioendothelioma, Kaposi's sarcoma, others
Malignant
Angiosarcoma
Epithelioid hemangioendothelioma
Malformations
Simple (i.e., venous, lymphatic, capillary, and arterial)
Combined: defined as two or more vascular malformations found in one lesion
Associated with other syndromes: Klippel-Trenaunay syndrome, Parkes Weber syndrome, etc.

Modified from ISSVA [6]
[a]Rapidly involuting (RICH), noninvoluting (NICH), partially involuting (PICH)

Table 16.3 Equivalence in terminology between the two main classification systems for vascular lesions

WHO classification	ISSVA
Cavernous hemangioma	Venous malformation
Venous hemangioma	Venous malformation
Intramuscular hemangioma	Venous malformation (mainly)
Lymphangioma	Lymphatic malformation (localized)
Lymphangiomatosis	Lymphatic malformation (diffuse)
Arteriovenous hemangioma	Arteriovenous malformation
Capillary hemangioma	Infantile hemangioma

Modified from Refs. [4, 11–13]

Therefore, we will use this classification in this chapter; however, Table 16.3 [4, 11–13] indicates comparison between the two classification systems.

Other entities, such as glomus tumors and synovial hemangiomas, will be discussed separately.

16.3 Vascular Tumors

16.3.1 Benign Vascular

We will only describe the most common lesions and those associated with clinical or specific nosological entities.

16.3.1.1 Infantile Hemangioma (IH)

Infantile hemangiomas are the most common vascular tumor of infancy [10]. They occur three to five times more frequently in females compared to males [14] and may be present at birth but are frequently diagnosed by 3 months of age [10]. In most cases, diagnosis is made clinically through the observation of a subcutaneous bluish red mass that looks like the surface of a strawberry (Fig. 16.1).

These tumors undergo two biologic phases:

- *The proliferative phase*, which is characterized by rapid endothelial growth in the first few months of life that stabilizes in size at approximately 9–10 months of age. Reflecting the characteristic high-flow component of this phase, the tumor manifests as a pulsatile and warm mass [15].
- *The involuting phase*, which occurs over the next several years, is a period during which the hemangioma spontaneously decreases in

Fig. 16.1 Proliferative infantile hemangioma in a 15-month-old boy. Clinical photograph shows a diffuse and lobulated mass in the arm with superficial involvement, which causes its strawberry-like appearance

size and is replaced by a residual fibrofatty mass [16]. This process is usually completed by 7–10 years of age [17].

On pathological examination, whatever the phase, IHs express a unique immunophenotype (glucose transporter protein-1 (GLUT1)), which differentiates them from other vascular lesions [18].

Infantile hemangiomas are most commonly seen on the face and neck (60 % of cases), followed by the trunk (25 %) and extremities (15 %) [19]. They are multifocal in approximately 30 % of the cases [1].

During the proliferative phase, the lesion appears as a well-defined mass with variable echogenicity. The vessels may be visible using US. Doppler demonstrates a characteristic hypervascular lesion with a high density of vessels (arteries and veins) and a low resistance on spectral analysis (Fig. 16.2) [2, 20]. Despite the high-flow nature of the lesion during this phase, there is a distinct soft tissue lesion that usually contains a single afferent artery and no direct arteriovenous shunting, unlike arteriovenous malformations [2]. During the involuting phase, IHs appear hyperechoic with a low density of vessels.

The appearance of IHs using MR imaging is indicative of their biologic phase. The proliferative phase is characterized by a well-circumscribed lobulated lesion with low or iso-signal intensity on the T1-weighted images and a high signal intensity on the T2-weighted images; the IH lesions also show an early and homogeneous enhancement after gadolinium administration (Fig. 16.2) [21]. Fast-flow vessels appearing as flow voids can be depicted within and around the lesion [2]. During the involuting phase, the increasing amount of fat within the tumor increases the signal intensity of the lesion on the T1-weighted images, which is associated with less avid contrast enhancement (Fig. 16.3).

The presence of a high resistance index on the spectral analysis or a marked perilesional edema on the T2-weighted images is suggestive of other tumoral lesions, such as sarcomas, neuroblastomas, myofibromatosis, tuft hemangiomas, metastatic neuroblastomas, or other tumors [2].

Multiple hemangiomas of the skin are usually linked with visceral hemangiomas. Segmental hemangiomas may be associated with PHACE syndrome (see Sect. 16.6.1) [22]. Most of these segmental hemangiomas are telangiectatic or reticular and do not demonstrate a high-flow pattern on Doppler US.

In the majority of the cases, no treatment is required due to spontaneous involution. However, 10–20 % of the cases require treatment, including cases with periocular location with vision compromise, high-output cardiac failure, ulceration, compression of the airway, facial hemangiomas with rapid growth and distortion, and symptomatic muscular hemangiomas. Medical treatment is usually attempted first, and propranolol is typically the first-line therapy with excellent results in most cases [23]. Other treatments include corticosteroids, vincristine, interferon, and laser therapy. Surgery is required when medical alternatives are ineffective, mostly in cases involving function-threatening, life-endangering, and disfiguring lesions [16].

Key Points

1. Infantile hemangioma.
2. The most common vascular tumor of infancy.
3. Characterized by two biologic phases (proliferative/involuting).
4. Positive for the GLUT1 marker at both stages.
5. Presence of a high-flow soft tissue mass.
6. If perilesional edema is present, other tumoral lesions must be ruled out.

16.3.1.2 Congenital Hemangioma (CH)

CHs are rare and fully developed at birth; therefore, they are potentially seen in utero. Three subtypes have been identified [6, 24, 25]:

– Rapidly involuting congenital hemangiomas (RICH), which completely regress during the first 2 years of life.
– Noninvoluting congenital hemangiomas (NICH), which demonstrate growth propor-

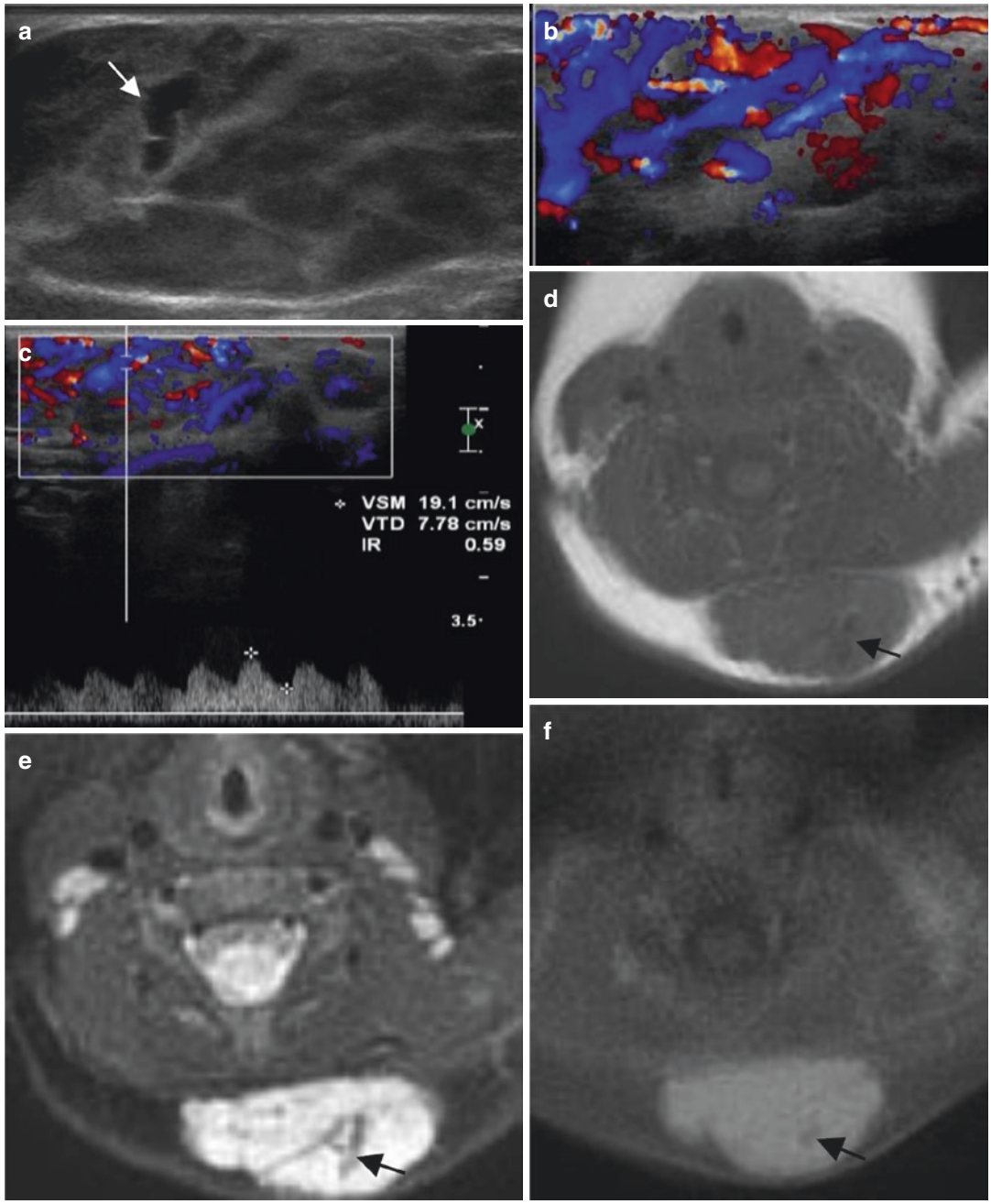

Fig. 16.2 Infantile hemangioma. Nine-month-old boy with subcutaneous mass in his posterior cervical neck. (**a**) Axial Ultrasound. (**b**) Axial color Doppler ultrasound. (**c**) Spectral analysis obtained in tumor center. (**d**) Axial T1-weighted MR image. (**e**) Axial T2-weighted MR image, with fat suppression. (**f**) Axial T1-weighted MR image after Gadolinium contrast administration with fat suppression. (**a–c**) Ultrasound shows a solid mass with well-defined margins in the subcutaneous soft tissues of the neck (**a**). The lesion is predominantly hyperechoic with scattered hypoechoic foci that correspond to vessels (*white arrow*). (**b**, **c**) Color Doppler shows hypervascular lesion with low-resistance arteries. (**d–f**) MRI shows a well-defined, lobulated soft-tissue mass confined to the subcutaneous soft tissues. The mass is isointense relative to muscle on the unenhanced T1-weighted image (**d**), hyperintense on T2-weighted image (**e**), and shows uniform enhancement (**f**). All three images demonstrate small, intralesional signal void foci (*black arrows*) due to fast flow vessels. There is no invasion of the underlying muscle and no perilesional oedema

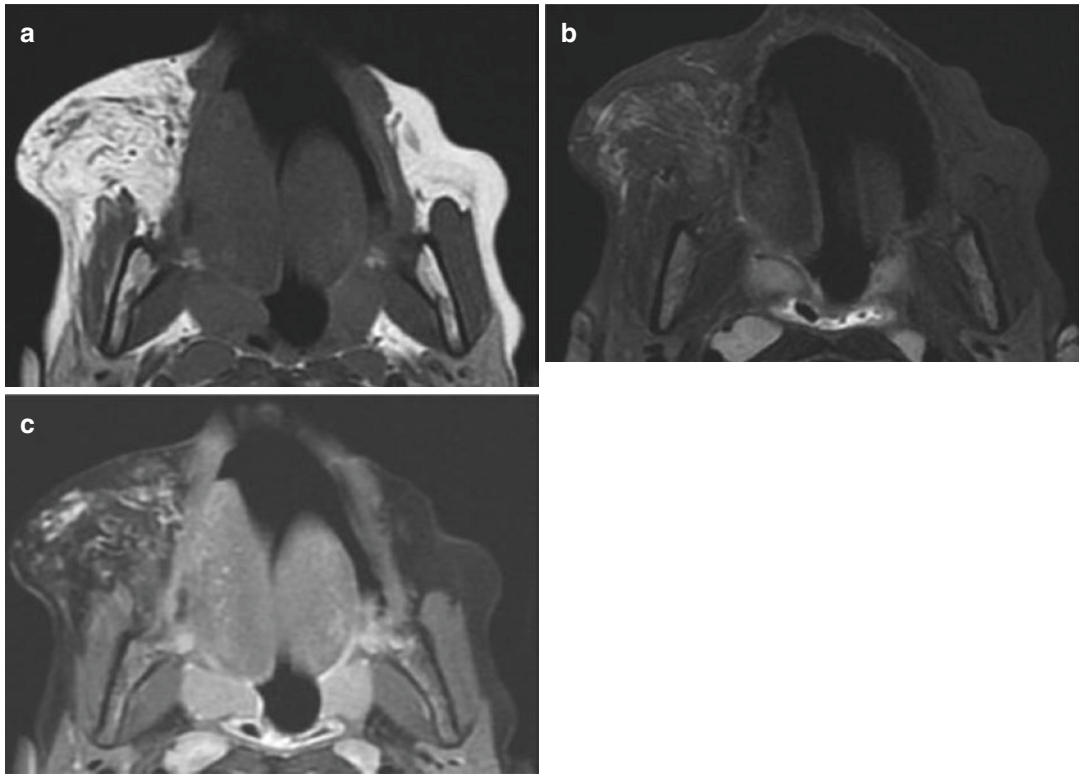

Fig. 16.3 Infantile haemangioma of the cheek in a 7-year-old girl during involution phase. (**a**) Axial T1-weighted MR image. (**b**) Axial T2-weighted MR image with fat suppression. (**c**) Axial T1-weighted MR image after Gadolinium contrast administration with fat suppression. MRI images show a subcutaneous hyperintense mass on T1-weighted image (**a**), slightly hyperintense on T2-weighted image (**b**) with minimal enhancement (**c**). No flow voids are seen

tional to that of the child without regression (Fig. 16.4).

– Partially involuting congenital hemangiomas (PICH), which have a distinct behavior, evolving from RICH to NICH-like lesions. RICH may be clinically difficult to differentiate from infantile hemangioma but the GLUT1 marker is negative.

Congenital hemangiomas share the same imaging findings on sonography. These features are similar to those of infantile hemangiomas, except for the presence of intravascular thrombi, vascular aneurysms, and arteriovenous shunting [26].

NICH are usually treated by a surgical resection [27].

16.3.1.3 Epithelioid Hemangioma

This benign vascular tumor is encountered in adult patients with a variable sex predilection [5, 28]. It is usually superficially located and is responsible for red nodules mainly on the face and fingers. Furthermore, deep locations, including in the bone, are possible [5]. Epithelioid hemangiomas are differentiated from Kimura's disease, a chronic inflammatory lesion affecting young Asian men, which shares clinical and pathological similarities to epithelioid hemangiomas [29]. The imaging is nonspecific [28].

16.3.2 Intermediate and Malignant Vascular Tumors

16.3.2.1 Kaposiform Hemangioendothelioma (KHE)

KHEs are locally aggressive, rare vascular tumors of intermediate malignancy [5, 6]. Their

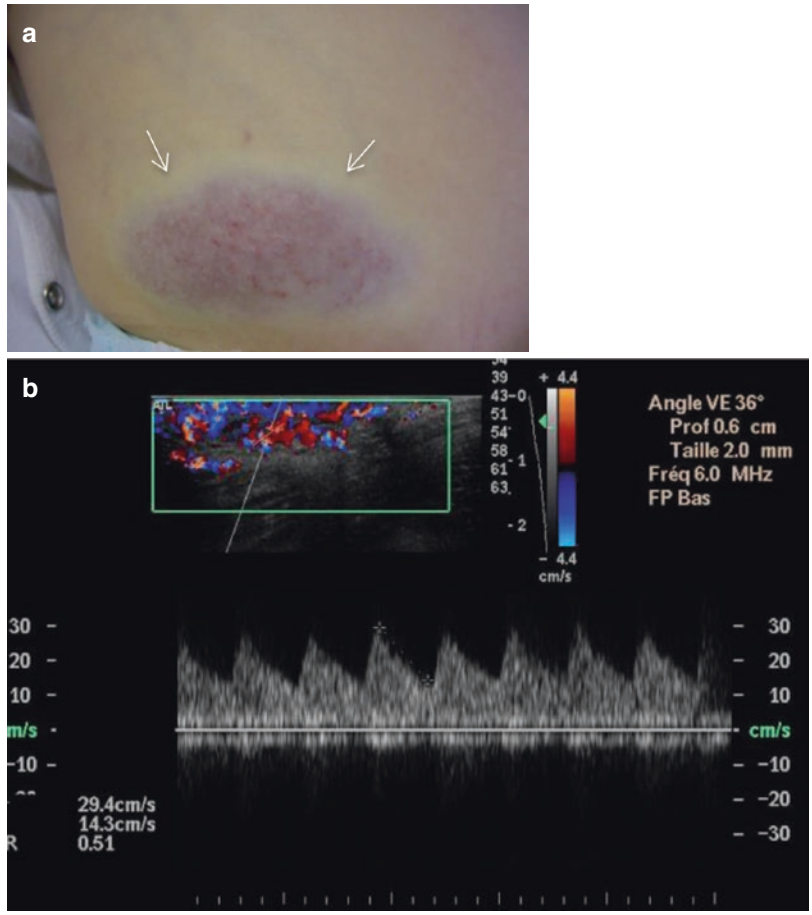

Fig. 16.4 Congential hemangioma in a 3-year-old boy. (**a**) Clinical photograph. (**b**) Axial color Doppler image with spectral display obtained in tumor center. (**a**) Non-involuting congenital hemangioma (NICH) is seen as an overlying bluish discoloration with clear peripheral halo (*arrow*). The lesion has been present since birth, growing proportionally to the patient's growth. (**b**) Color Doppler image shows the marked increased vascularity inside the lesion with low-resistance arteries. The imaging features are indistinguishable from those of infantile hemangioma

pathology is characterized by frequent lymphatic abnormalities [10]. Even if the tumor does not metastasize, intra-abdominal deep forms have a poor prognosis because they are rarely curable by surgery [30].

MR imaging helps to differentiate KHEs from infantile hemangiomas. KHE appears as an ill-defined lesion with hemosiderin deposits and smaller feeding and draining vessels. Moreover, KHEs involve multiple tissue planes and destruction of the adjacent bones is also observed [10, 15].

KHEs are often associated with Kasabach-Merritt syndrome [10] which is characterized by thrombocytopenia, microangiopathic hemolytic anemia, and localized consumption coagulopathy. In the latter case, medical treatment is recommended (propranolol, corticosteroids, vincristine) [31, 32].

16.3.2.2 Kaposi's Sarcoma

Kaposi's sarcoma (KS), also known as KS-associated herpesvirus (KSHV), is a locally aggressive vascular tumor associated with the human herpesvirus-8 (HHV-8). This tumor is probably of lymphatic origin and is characterized by neoangiogenesis and proliferation of spindle-shaped cells with inflammation and edema [33]. It is usually a multicentric disease that originates

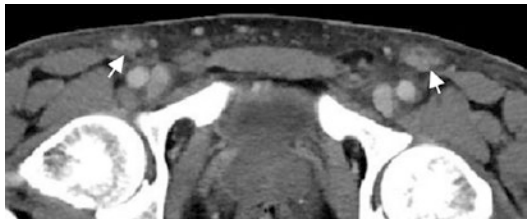

Fig. 16.5 Kaposi sarcoma in a 35-year-old man (endemic type). Computed tomography after iodinated-contrast injection shows an enhancing bilateral inguinal lymphadenopathy (*arrows*)

in the lymphoreticular system and may involve the skin, lymph nodes, lungs, gastrointestinal tract, liver, spleen, and musculoskeletal system. Four types of KSs have been described: classic KS (chronic form, patients older than 60 years old), endemic KS (middle-aged adults and children, African KS), KS in iatrogenically immunosuppressed patients (related to solid organ transplantation or immunosuppressive therapy), and AIDS-related KS [28, 33]. The topography of the lesions and their aggressivity depend on the type of KS. For example, KS AIDS is often aggressive and multifocal (face, genitals, lung, lower extremities). Imaging depends on the location of the lesion and the lymph nodes are typically hypervascular (Fig. 16.5) [28, 33].

16.3.2.3 Epithelioid Hemangioendothelioma (EH)

This rare malignant vascular tumor demonstrates a local recurrence rate of 10–15 % and a high metastatic rate (20–30 %). About half of the cases are multifocal [34, 35]. This lesion can arise in any vascular tissue and has been reported to be located on the skin, muscle, vasculature, bone, brain, and stomach. Tumor location in the liver and lungs may be confused with metastatic disease [35–37]. The adjacent vessels may be thrombosed, which may lead to symptoms. Calcifications can be observed [36, 38]. This lesion is often associated with Kasabach-Merritt syndrome.

16.3.2.4 Angiosarcoma

Angiosarcoma is a high-grade malignant tumor with a high mortality rate [39]. It may involve the skin (33 % of the cases), the deeper soft tissues (24 % of the cases), the internal organs, or the bones [38]. The presence of chronic lymphedema (Stewart-Treves syndrome) occurs in approximately 10 % of the cases and is a well-known risk factor for angiosarcoma [38]. Stewart-Treves syndrome is usually reported in the upper extremities after a mastectomy for breast cancer. Additionally, it can be seen in the lower extremities after hysterectomy for uterine cancer, trauma, or infection [40]. Angiosarcoma is rarely radiation-induced, and it exceptionally arises in vascular lesions [41]. Clinically, two types of angiosarcoma can be seen:

- A cutaneous form (purplish red plate, possibly nodular)
- A deep form (painful soft tissue mass in the lower limbs) [5, 39]

Metastasis most frequently involves the lung and lymph nodes, followed by the liver, the bones, and the soft tissues [39]. The imaging appearance depends on whether the lesion is located superficially or deep. Skin thickening or focal soft tissue nodules are observed when the lesion involves the skin and subcutaneous tissues. The imaging features are not specific and include intermediate echogenicity, variable signal intensity on T2-weighted images, and variable contrast enhancement (Fig. 16.6) [28]. When the lesion is associated with chronic lymphedema, extremity enlargement, diffuse skin thickening, and edema of the subcutaneous connective tissue can be seen (Fig. 16.7).

16.4 Vascular Malformations

Vascular malformations are defined by an abnormal vasculogenesis with a normal turnover of endothelial cells. They are subcategorized according to their hemodynamics [42]:

- Low-flow malformations (venous, lymphatic, capillary, capillary-venous, and capillary-lymphatic-venous)
- High-flow malformations (arteriovenous malformations [AVMs] corresponding to an

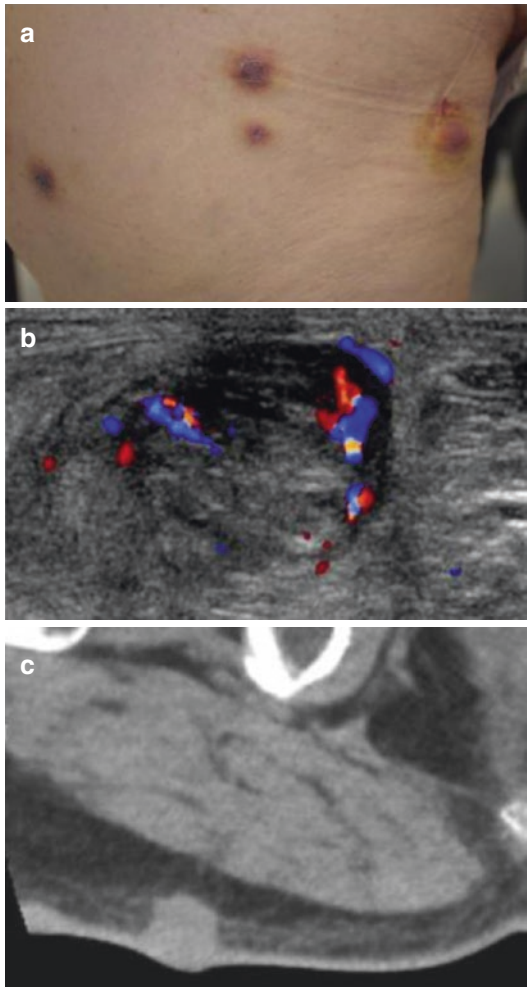

Fig. 16.6 Angiosarcoma in a 70-year-old men. (**a**) Clinical photograph. (**b**) Axial color Doppler image. (**c**) Computed tomography. (**a**) Clinical appearance of numerous skin lesions. (**b**) Ultrasound with color Doppler shows nodular superficial tissue mass, slightly hypoechogenic and predominately peripheral flow within the soft tissue mass. (**c**) Computed tomography demonstrates a non specific subcutaneous nodular lesion

anastomosis between an artery and a vein through a nidus and arteriovenous fistulas [AVFs] with a direct anastomosis between a main artery and a main vein)

This distinction is important for planning treatment. Interventional radiologists play a major role in these lesions with the increasing use of sclerotherapy and embolization therapies.

16.4.1 Venous Malformations (VMs)

VMs represent the most common peripheral vascular malformation [43, 44]. They can be simple, combined (e.g., capillary-venous and capillary-lymphaticovenous malformations), or syndromic (associated with Klippel-Trenaunay syndrome, blue rubber bleb nevus syndrome, or Maffucci syndrome). They are present at birth, but patients usually develop symptoms during late childhood or early adulthood (especially during puberty and pregnancy). They vary in size and shape and can be localized and well defined or diffuse and infiltrative. They can involve the superficial and/or deep tissues. When superficial, patients typically demonstrate bluish skin abnormalities and a soft compressible and nonpulsatile soft tissue mass [45]. They typically expand during the Valsalva maneuver and decompress with extremity elevation and local compression [17, 45]. They can also be deep, involving many anatomical structures, including the muscle, synovial membrane, bone, and liver [4, 45, 46]. They may cause pain, impaired mobility, and skeletal deformities. They are usually located on the extremities (40%), head and neck (40%), and trunk (20%) [17, 45]. Elevated D-dimer levels are a specific biomarker for VMs [47].

Pathologically, VMs are characterized by small- or large-sized venous channels connected with the normal venous system. They may contain thrombi whose dystrophic mineralization produces phleboliths [43]. Although pathologists now apply the new ISSVA nomenclature [46, 48], the historical terminology is kept in the current WHO classification (Table 16.1) [5]. Therefore, entities such as cavernous, venous, or intramuscular hemangiomas usually correspond to venous malformations and are still frequently used in pathologic reports using the WHO classification [5, 38, 46].

Phleboliths and dystrophic calcifications are easily detected on radiographs and CT and are highly suggestive of VMs (Fig. 16.8) [2]. In case of extensive malformations, the involvement of the adjacent joints or bones is possible, such as cortical erosion, periosteal reaction, regional osteopenia, and bony overgrowth [49, 50].

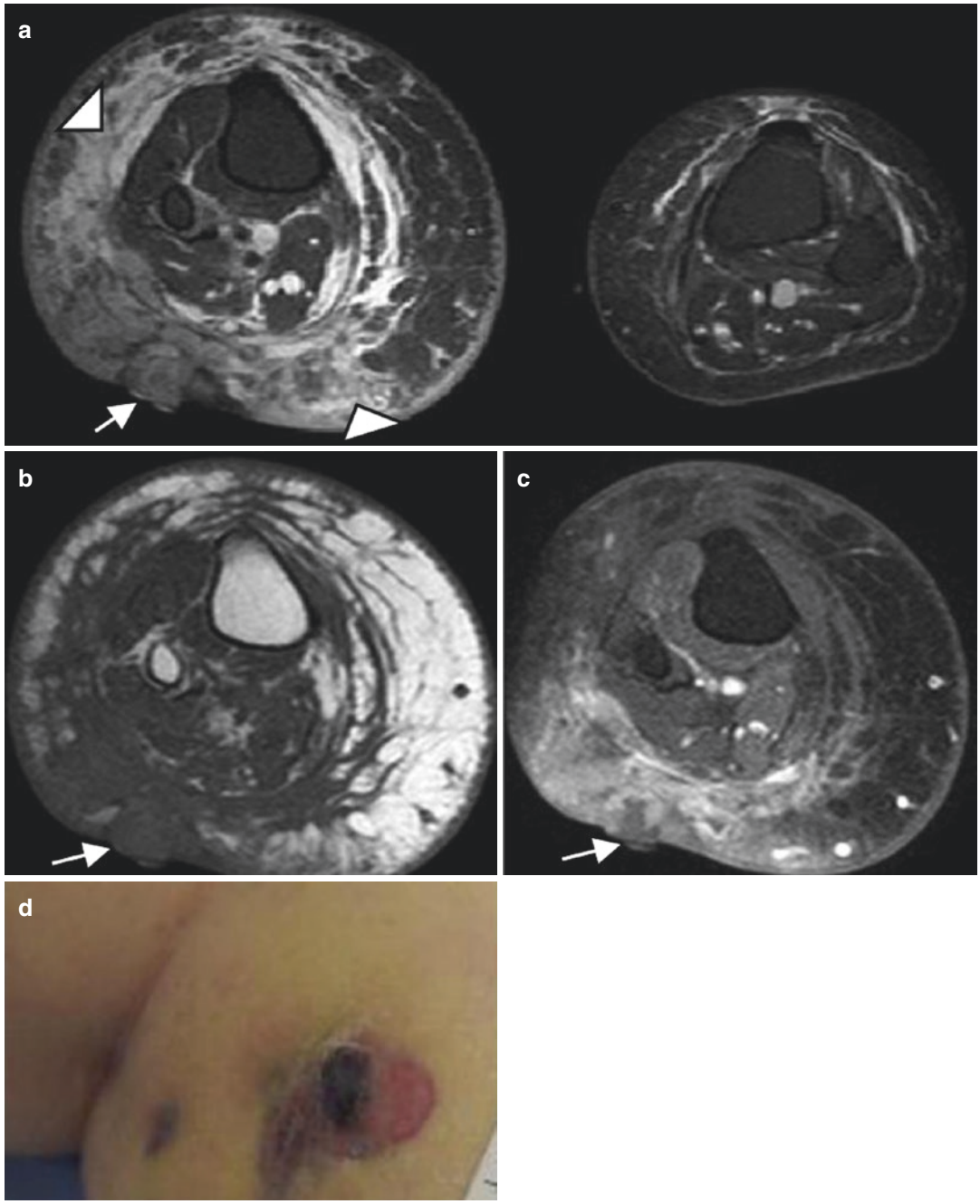

Fig. 16.7 Stewart-Treves syndrome in a 66-year-old woman who was treated 20 years ago for uterus cervical cancer. (**a**) Axial T2-weighted MR image, with fat suppression. (**b**) Axial T1-weighted MR image. (**c**) Axial T1-weighted MR image after Gadolinium contrast administration, with fat suppression. (**d**) Clinical photograph. (**a**) Axial T2-W fat-suppressed MR images reveals an enlarged right extremity with subcutaneous edema (*arrowheads*) (**a**–**c**) Nodular mass of low signal intensity on T1, with low to intermediate and heterogeneous signal intensity on T2 and a heterogeneous enhancement (*arrows*) representing the angiosarcoma. (**d**) Clinical photograph shows the purplish skin lesion

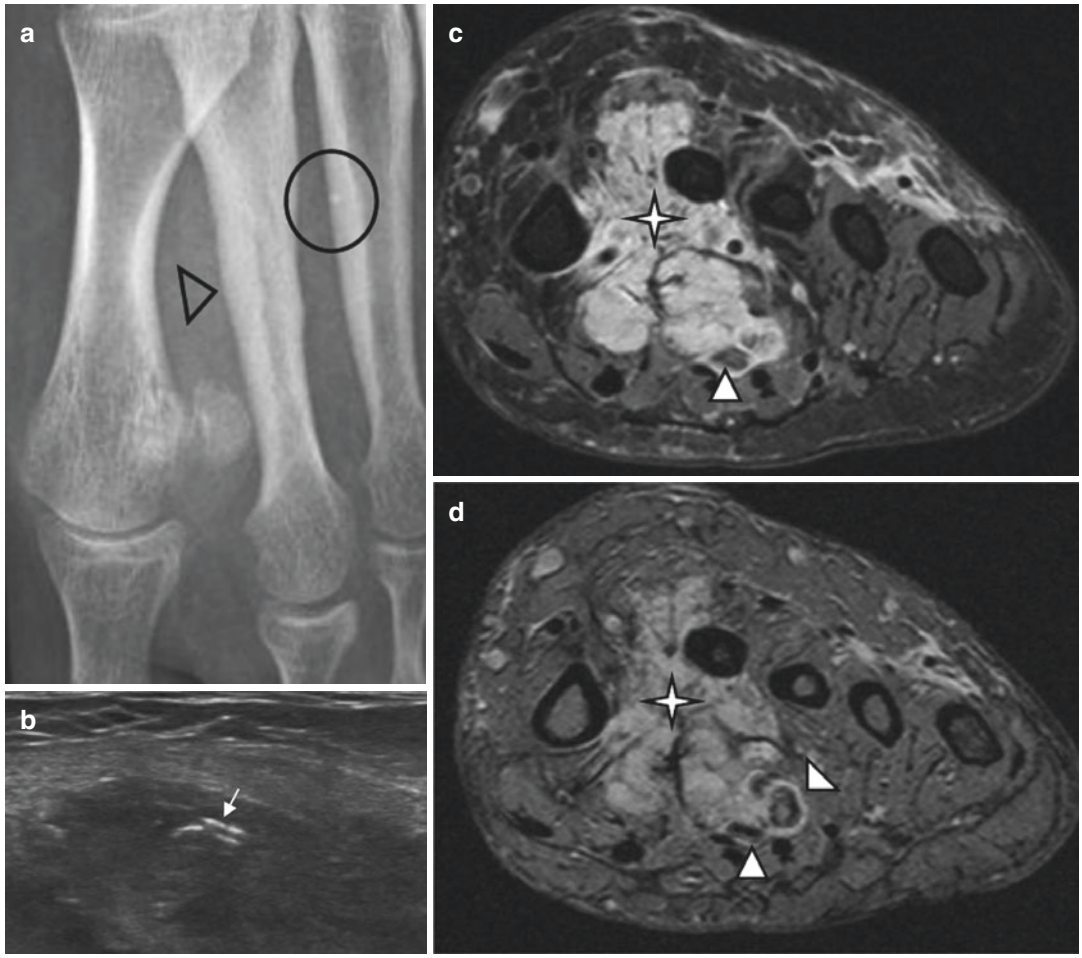

Fig. 16.8 Venous malformation of the left plantar region. (**a**) Plain radiograph. (**b**) Axial ultrasound. (**c**) Axial spin-echo T2-weighted MR image, with fat suppression. (**d**) Axial gradient-echo T2-weighted MR image. (**a**) Plain radiography demonstrates periosteal reaction, probably related to chronic vascular stasis (*black arrowhead*), and phlebolith (*circle*). This finding is characteristic of intramuscular venous malformation. (**b**) US shows hypoechogenic soft-tissue lesion with hyper echogenic foci with posterior acoustic shadowing corresponding to phleboliths (*arrow*). (**c**, **d**) Spin-echo and gradient-echo T2-weighted images show the VM as multiple slightly hyperintense serpiginous channels (*star*) with rounded hypointense phleboliths (*white arrowheads*), extending within the plantar muscles

Ultrasound shows an extremely variable appearance of the lesion, ranging from predominantly solid to multicystic lesions [1]. VMs can be well defined or infiltrative. These usually hypoechoic and heterogeneous lesions consist of tubular vascular or cavity compressible areas, reflecting the presence of vessels. The phleboliths are usually seen as hyperechoic foci. After applying compression, the movement of blood into the cavities can be identified (Fig. 16.9). Doppler US typically shows no flow or low-velocity flow. In the absence of a spontaneous vascular signal, dynamic maneuvers such as the Valsalva maneuver or manual compression by the probe followed by its decompression can cause the appearance of vascular signal although thrombosis is possible.

MRI is an excellent imaging modality to define the extent of the lesions and their relationship with the adjacent structures. VMs demonstrate well- or ill-defined limits, but they typically do not produce any significant soft tis-

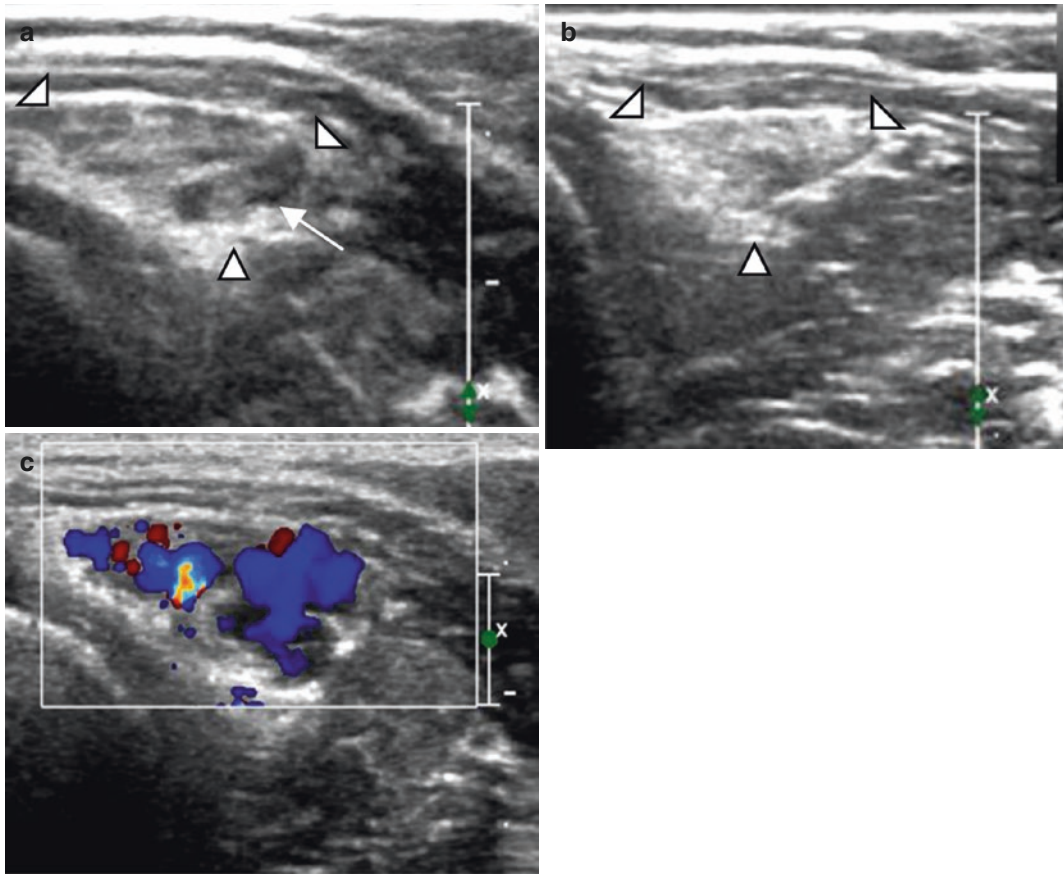

Fig. 16.9 Five-year-old girl with intramuscular venous malformation. (**a**) Ultrasound image. (**b**) Ultrasound image after local compression. (**c**) Color Doppler image. (**a**) Ultrasound image shows a heterogeneous lesion (*arrowhead*) with internal fluid component (*arrow*). (**b**) The lesion is compressible (*arrowhead*). (**c**) After decompression, filling of the cavities (vessels) can be observed on color Doppler US

sue mass syndrome, which suggests diagnosis. Vascular vessels are seen as tubular and serpiginous cavities with hypo- to iso-signal intensity on T1-weighted images and strong hyper-signal intensity on T2-weighted images, separated by hyperechoic fat (Fig. 16.10). Fat-suppressed T2-weighted images are particularly useful to evaluate the extent of the VMs. Phleboliths appear as small low-signal-intensity foci on all pulse sequences. Sometimes fluid-fluid levels due to hemorrhage or high protein content can be seen (Fig. 16.11) [1], though they are less common compared to lymphatic malformations. Contrast-enhanced 3-D acquisitions after dynamic gadolinium administration should be performed to evaluate the perfusion of the malformation and its drainage into the venous system. VMs are characterized by a lack of arterial and early venous enhancements and the absence of enlarged feeding vessels or arteriovenous shunting. They typically demonstrate a slow and progressive enhancement. Characteristic nodular enhancement of tortuous vessels can be observed on delayed venous phase images (Fig. 16.12) [3, 51]. The time between the beginning and the maximal enhancement is between 50 and 100 s [52]. Less specific appearances may be encountered when the lesion is composed of small vessels (Fig. 16.13) or in the absence of adipose tissue [53]. Intramuscular VMs often demonstrate serpiginous venous channels between the muscle

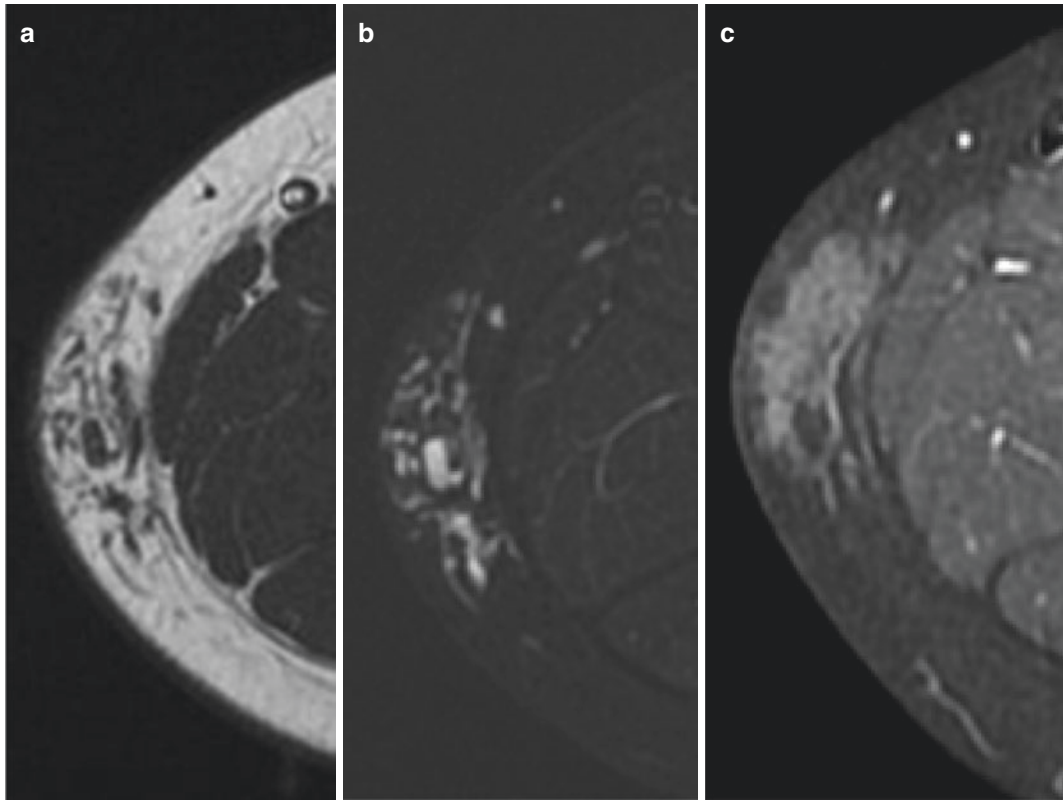

Fig. 16.10 Ten-year-old boy with subcutaneaous venous malformation. (**a**) Axial T1-weighted MR image. (**b**) Axial T2-weighted MR image with fat suppression. (**c**) Axial T1-weighted MR image after Gadolinium contrast administration with fat suppression. (**a**) MR images show multiple serpiginous areas confined to the subcutaneous soft tissues, isointense on T1-weighted image, separated by hyperintense areas corresponding to fatty components. (**b**) The lesion is hyperintense on T2-weighted image and (**c**) shows diffuse enhancement

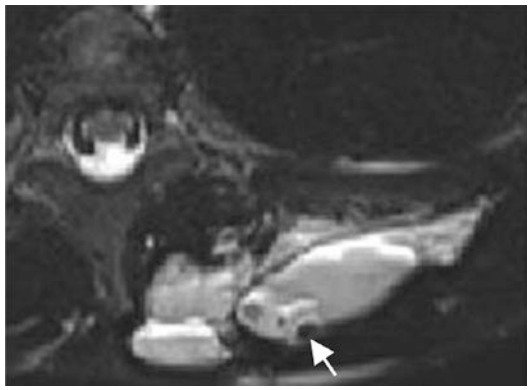

Fig. 16.11 Venous malformation with fluid-fluid level in a 5-year-old boy with recent trauma. Axial T2-weighted MR image with fat suppression reveals numerous intramuscular cavities with fluid–fluid levels. Note the presence of low signal intensity spot corresponding to phlebolith

fibers that are oriented along the long axis of the involved muscle [1]. Intra-articular involvement may lead to chronic hemarthrosis and joint destruction [54, 55] (Fig. 16.14). Localized intravascular coagulopathy is more frequent in diffuse compared to focal VMs and can be responsible for pain and thrombosis [56].

Most VMs are managed conservatively with a compression bandage of the extremity and medical antalgics for pain. In cases of major pain, joint involvement, and functional or cosmetic problems, the first-line treatment for VMs is sclerotherapy (dehydrated ethanol, sodium tetradecyl sulfate, polidocanol, and bleomycin), which can be followed by resection, laser therapy, and photodynamic therapy [57, 58].

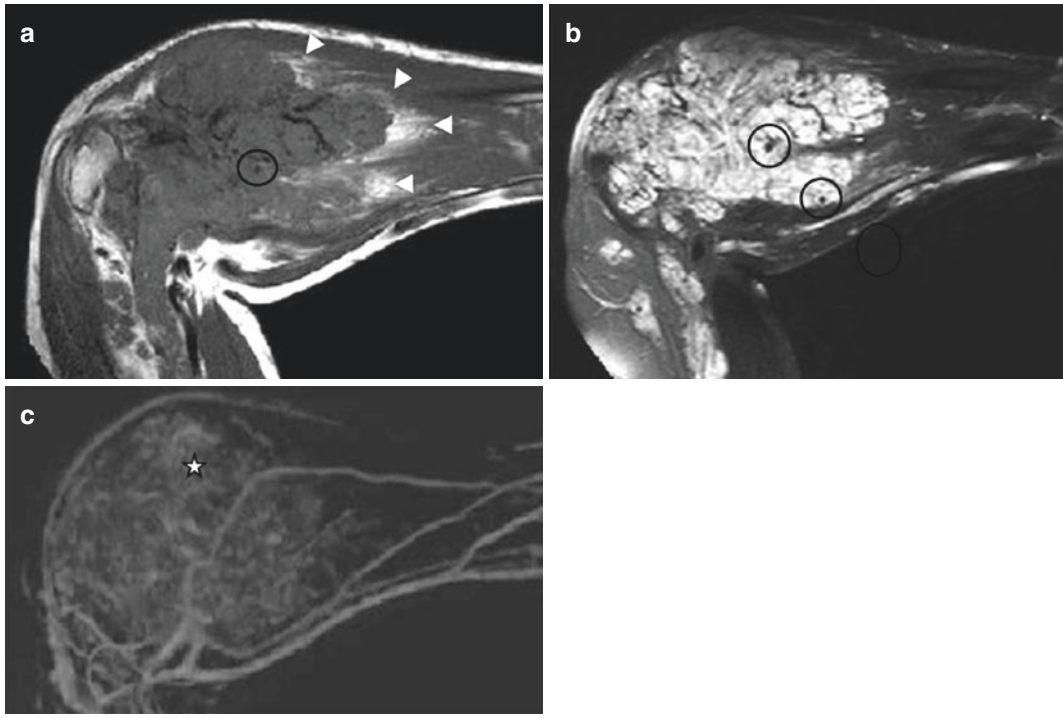

Fig. 16.12 Intramuscular venous malformation of the upper extremity. (**a**) Sagittal T1-weighted MR image. (**b**) Sagittal T2-weighted image with fat saturation. (**c**) Maximum intensity projection (MIP) after 3D contrast-enhanced MR angiography, late venous phase. (**a**) T1-weighted image shows an intramuscular and extensive lesion which involves the forearm muscles and elbow joint, surrounded by fat component (*arrowheads*). (**b**) The lesion is composed of multiple tortuous hyperintense vessels on T2-weighted image representing a slow flow vascular malformation. At least two phleboliths (*circles*) are seen as low signal foci inside the dilated veins. (**c**) Late venous phase image from gadolinium-enhanced 3D MR angiography shows characteristic filing of cavernous spaces with diffuse and nodular enhancement (*star*)

Key Points

1. Venous malformations
2. Superficial or deep (muscle, synovial membrane, bone, liver) and localized or diffuse
3. Expansion during Valsalva maneuver/decompression with extremity elevation and local compression
4. Phleboliths +++
5. Tubular and serpiginous cavities strongly hyperintense on T2-weighted images
6. Diffuse and delayed enhancement of the slow-flowing venous channels after contrast administration

16.4.2 Lymphatic Malformations (LMs)

LMs represent the second most common type of vascular malformation after venous malformations [59]. These low-flow vascular malformations are classified into three types depending on the size of the cystic cavities [1, 2, 45, 60, 61]:

- Macrocystic types (formerly cystic hygroma), with cysts >2 cm
- Microcystic types (formerly lymphangioma), with cysts between 1 and 2 cm
- Mixed types with capillary and/or venous malformations

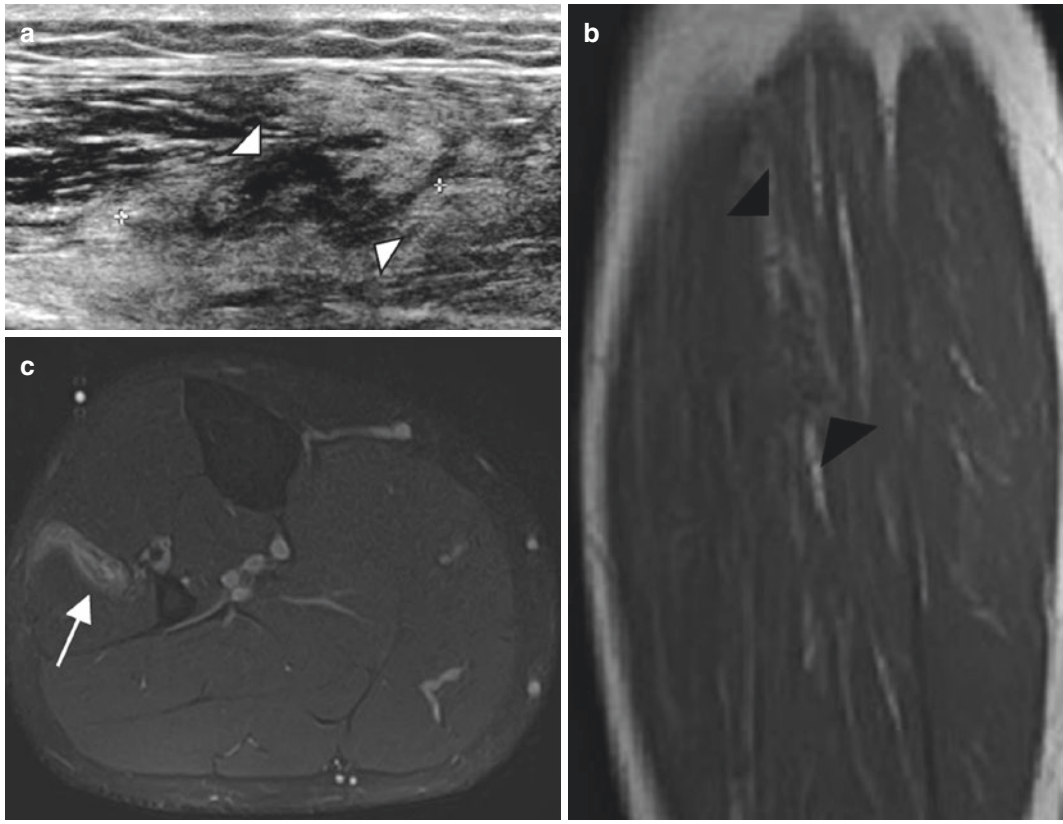

Fig. 16.13 Intramuscular venous malformation of the thigh in a 32-year-old man with pain exacerbated during exercise. (**a**) Ultrasound. (**b**) Sagittal T1-weighted MR image. (**c**) Axial T1-weighted MR image after Gadolinium contrast administration, with fat suppression (**a**) Ultrasound shows a nonspecific intramuscular soft tissue lesion (*white arrowhead*) (**b**) MR image demonstrates fat component surrounding the lesion (*black arrowheads*), (**c**) and serpiginous enhancement after gadolinium contrast administration (*arrow*)

Pathologically, they are composed of serpiginous dilated lymphatic channels that do not communicate with the normal lymphatic system [45], except in the retroperitoneum. Macrocystic and microcystic lesions are pathologically indistinguishable [61]. Diagnosis is suggested after a positive test for markers of lymph vessels, such as the vascular endothelial growth factor receptor 3 (VEGFR-3), LYVE-1, D2-40, and podoplanin [61–63]. However, it should be kept in mind that LMs can be associated with the other vascular malformations.

LMs are present at birth in half of the patients (prenatal diagnosis of macrocystic types is possible) and are diagnosed before the age of 2 years in 90% of the cases [61, 64]. They mainly involve the head and neck (55–95%) and axillary regions (20%) with a predilection for the left side of the body [64]. They can affect multiple structures (lung, intestine, liver, spleen, etc.) including the bones [38]. Macrocystic LMs are typically large and clinically manifest as a soft swelling mass with a rubbery consistency. They are well limited and mobile under a normal skin [57, 64]. Transillumination confirms the liquid nature of the lesion. The majority of the cases are asymptomatic, but complications, such as local compression, sudden increase in size secondary to bleeding (trauma), or infection from an adjacent process of the head and neck, can occur [65].

Microcystic LMs tend to infiltrate the adjacent structures. They are sometimes associated with a particular skin damage (lymphangioma

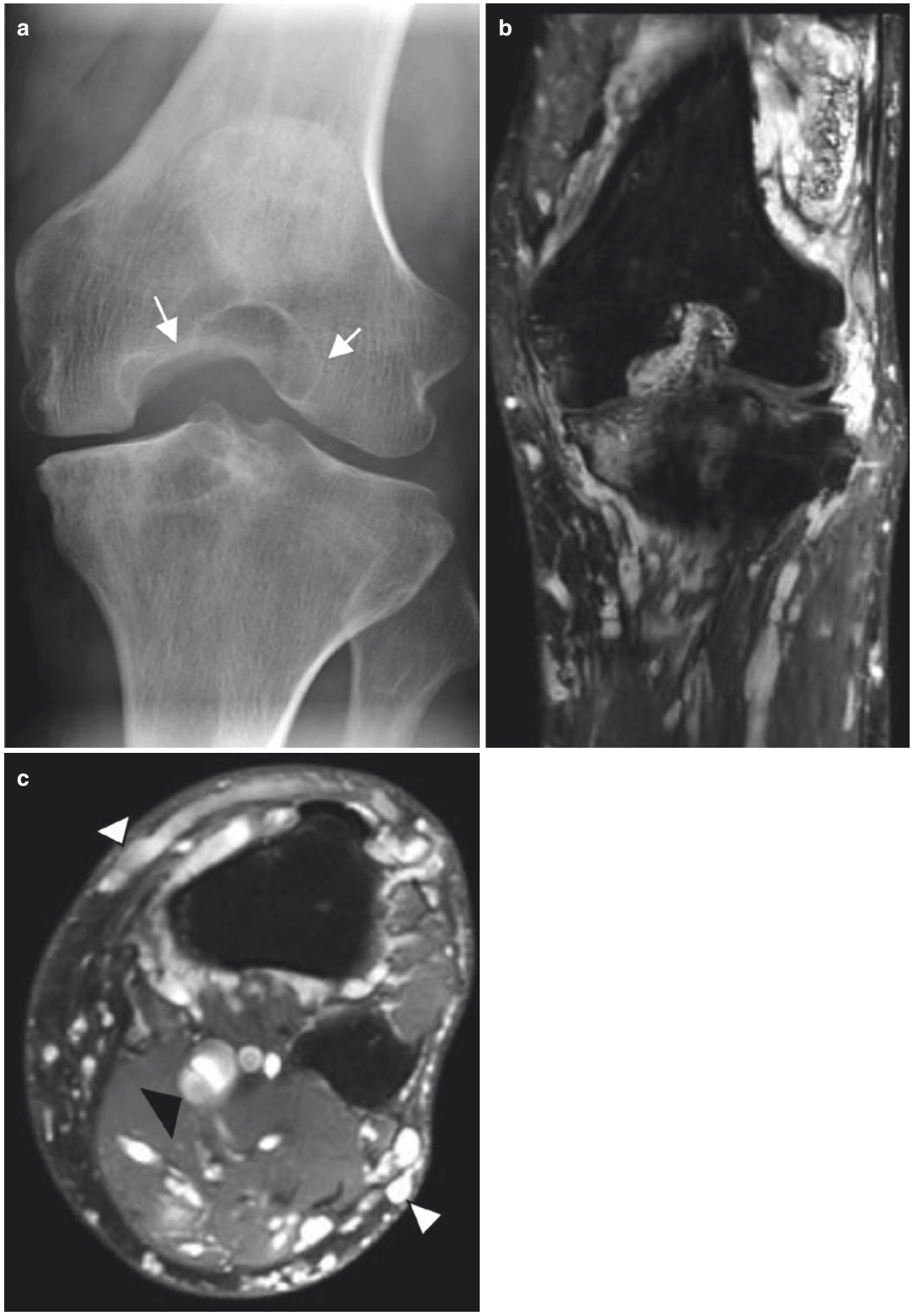
a
b
c

Fig. 16.14 Patient with diffuse and infiltrative venous malformation of the knee. (**a**) Plain radiograph. (**b**) Coronal T2-weighted image with fat saturation. (**c**) Axial T2-weighted image with fat saturation. (**a**) Plain radiograph shows a widening of intercondylar notch with erosion of the medial femoral condyle. (**b**, **c**) MRI shows infiltrative and serpentine vascular spaces with involvement of multiple compartments of the knee. Hyperintense nodular and serpentine areas of vascular vessels are seen in the subcutis (*arrowheads*), muscles and joint. Note the dilated deep veins (*black arrowhead*)

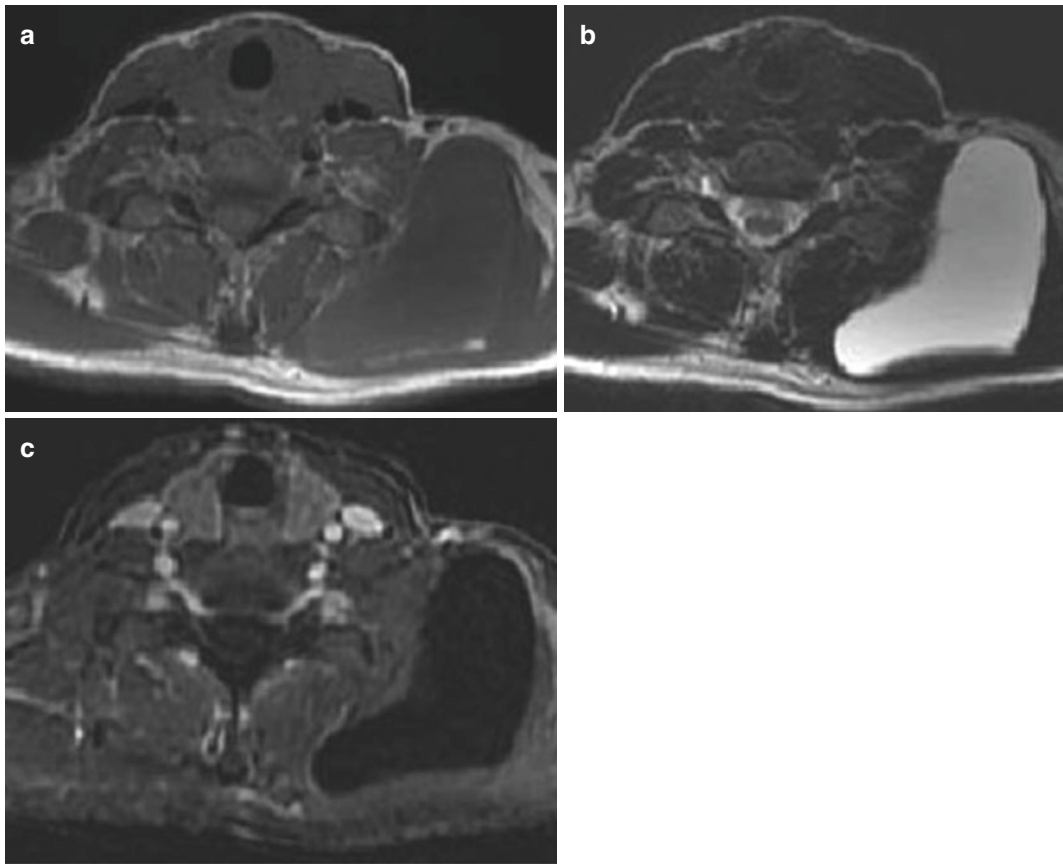

Fig. 16.15 Macrocystic lymphatic malformation in a 30-year-old woman with a swollen mass in the neck. (**a**) Axial T1-weighted MR image. (**b**) Axial T2-weighted MR image with fat suppression. (**c**) Axial T1-weighted MR image after Gadolinium contrast administration with fat suppression. (**a**) MRI demonstrates a well-defined, lobulated isointense mass on T1-weighted image, (**b**) which is highly hyperintense on T2-weighted image, (**c**) and does not enhance after gadolinium contrast administration

circumscriptum) [1, 2, 61]. More unusual locations include the mediastinum, retroperitoneum, omentum, mesentery, and bones [66].

Ultrasound demonstrates a multiloculated cystic mass and the size of the cavity determines the type of LM. The cystic spaces are mostly anechoic or hypoechoic, but levels may be observed in cases of bleeding, infection, or chylous fluid. Septa of variable thickness correspond to clusters of lymph structures. LMs do not demonstrate any associated vascularity, soft tissue components, or perilesional inflammatory changes. Calcifications are sometimes observed.

On MRI, LMs are usually seen as lobulated cystic masses with iso- to hypo-signal intensity on T1-weighted images and increased signal intensity on T2-weighted and STIR sequences (Fig. 16.15). Fluid levels can be observed in cases of superimposed hemorrhage or infection [3]. After contrast administration, macrocystic LMs

exhibit rim and septal enhancement [15, 44], whereas microcystic LMs do not show any enhancement (Fig. 16.16) [15]. However, combined lymphatic-venous malformations may show diffuse enhancement, which is related to the venous component enhancement in mixed malformations [3]. MRI is the best imaging modality to assess the exact extent of the lesion, which may

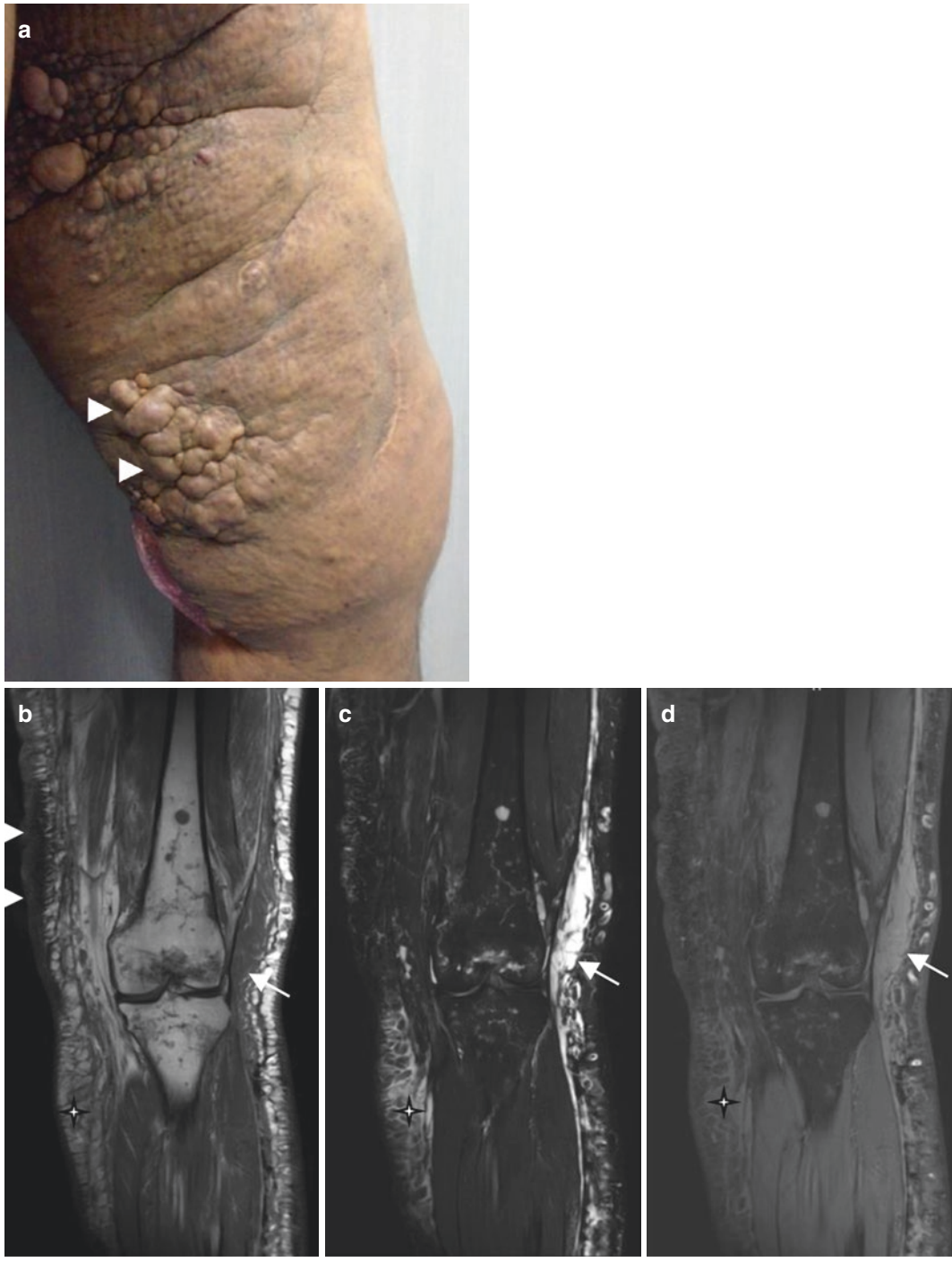

be localized or diffuse and very infiltrative [1]. Involvement of the adjacent bone may be present (Fig. 16.16). Needle aspiration confirms the diagnosis of LMs by finding lymphatic vessels.

The first-line therapy is percutaneous sclerotherapy, usually with absolute alcohol under radiological control. Several sessions are needed in extensive forms of LM. As this treatment is usually effective in macrocystic LMs, surgery is less frequently proposed [57]. Microcystic LMs are more difficult to treat and recurrence is more frequent. They should be managed conservatively as much as possible [2].

Key Points

1. Lymphatic malformations
2. Macrocystic, microcystic, or mixed
3. Most frequent in the neck and head regions and then axilla
4. Can be combined with other vascular malformations (capillary-venous)
5. Macrocystic LMs: cystic lesion/ring-septal enhancement after gadolinium contrast administration
6. Microcystic LMs: cutaneous skin damage/no significant enhancement after gadolinium contrast administration

16.4.3 Capillary Malformations (CMs)

These intradermal vascular lesions are composed of mature ectatic capillary channels and are hemodynamically inactive. The diagnosis of CMs is clinically based on the appearance of a cutaneous red discoloration [9]. CMs are present at birth in 0.3 % of children [15], and they typically regress. They usually involve the face but can develop anywhere. They can be associated with malformation syndromes, such as Sturge-Weber syndrome, Klippel-Trenaunay syndrome, and Parkes Weber syndrome. Nonspecific thickening of the skin can be observed with US or MRI [1].

16.4.4 Arteriovenous Malformations (AVMs)

AVMs are high-flow vascular malformations related to an abnormal communication between arteries and veins, with persistence of fetal capillary beds [8]. They are usually sporadic but can be seen in hereditary syndromes [26, 67]. They most often affect the head and neck region (including the brain), the extremities, and the internal organs [5]. They are present at birth in an early quiescent stage and usually do not become evident before until later childhood or adulthood. Like the other vascular malformations, they generally increase in size proportional to the growth of the child and are under hormonal influences (puberty, pregnancy). Their size can also be influenced by trauma (such as biopsy or incomplete surgery) [17, 45]. They are hemodynamically active, which can result in a red, pulsatile, warm mass with dilated superficial draining veins [68]. The presence of the shunt may induce limb hypertrophy and reflex bradycardia after compression of the lesion. Adjacent bone or joint damage is possible (marked periosteal reaction or destruction) [2, 26].

The histology of AVMs is highly variable with a combination of capillaries, venules, and arterioles in a fibrous or fibromyxoid stroma. Correlation with imaging is important for the diagnosis of AVMs. Calcifications and thrombosis are possible [5].

On US, AVMs are seen as ill-defined areas formed by multiple juxtaposed tortuous vessels, separated by hyperechoic fat. The vessels include arteries with diastolic flow and arterialized

Fig. 16.16 Microcystic lymphatic malformation. (**a**) Clinical photograph. (**b**) Coronal T1-weighted MR image. (**c**) Coronal T2-weighted MR image with fat suppression. (**d**) Coronal T1-weighted MR image after Gadolinium contrast administration with fat suppression. (**a**) Clinical photograph shows an extensive skin lesion of the thigh (*white arrowheads*). (**b**–**d**) MRI reveals the skin thickening on T1-weighted image (*white arrowhead*) (**b**) and a diffuse involvement of the subcutaneous tissue (*star*) with a lobulated and septated mass (*arrow*). There is no significant enhancement of these features (**d**), a finding characteristic of a microcystic lymphatic malformation. Note the associated involvement of the bone

draining veins with pulsatile flow (not seen in hemangiomas) [17]. The nidus is recognized by its various vascular areas and aliasing phenomena in terms of the color Doppler shunts [20].

MR imaging demonstrates tortuous structures composed of enlarged feeding arteries and draining veins without well-defined associated mass. Signal voids are observed in these vessels on both T1-W and T2-W SE sequences (Fig. 16.17), but high signal intensity is seen on gradient-echo sequences, indicating high-flow lesions [1, 45]. Gadolinium perfusion allows for the mapping of feeding arteries, draining veins, and the nidus [1]. Early venous filling is typically seen in AVMs (Fig. 16.18).

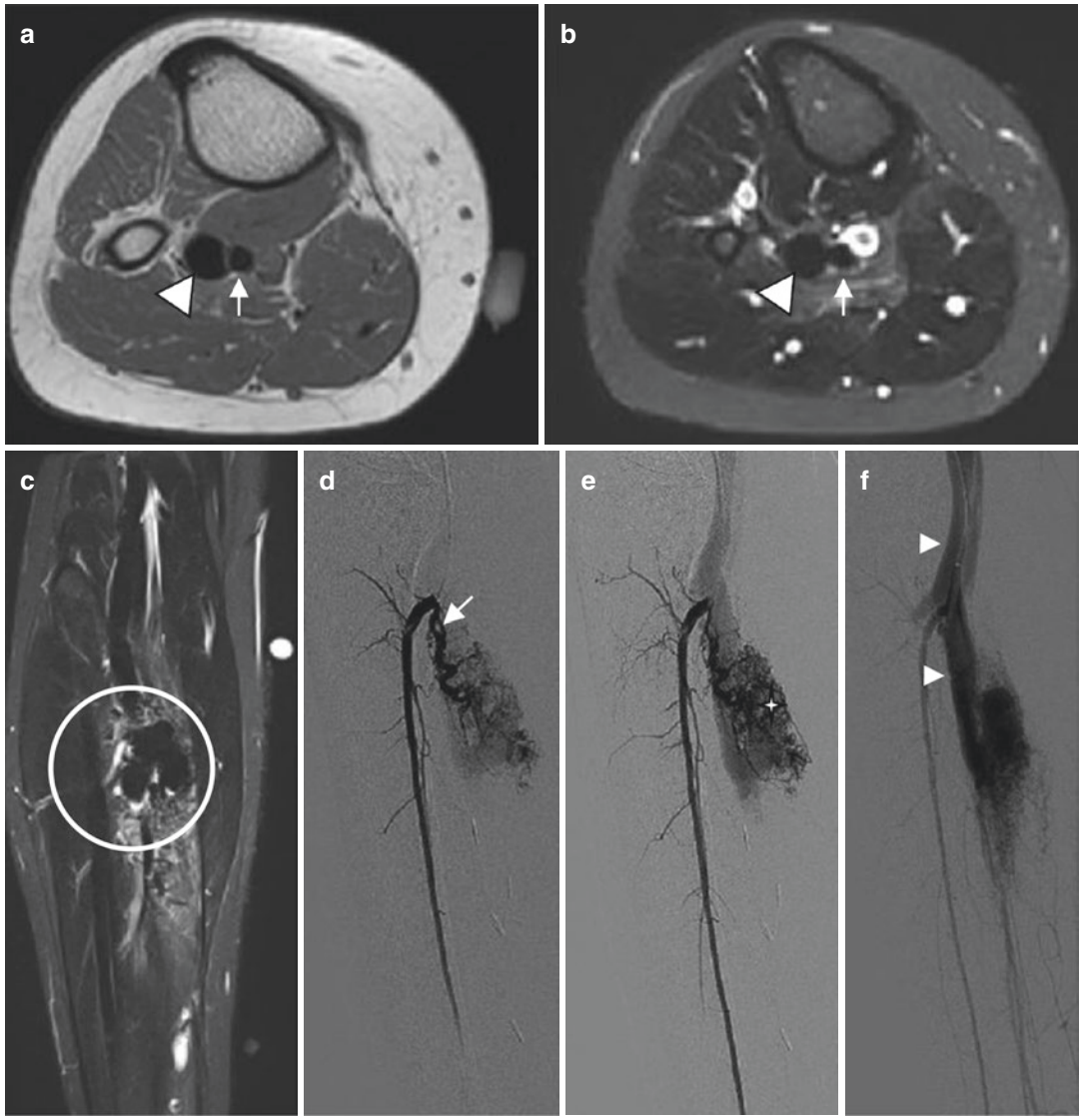

Fig. 16.17 Complex arteriovenous malformation affecting the calf in a 15-year-old woman. (**a**) Axial T1-weighted MR image. (**b**) Axial T2-weighted MR image with fat suppression. (**c**) Coronal T2-weighted MR image with fat suppression. (**d**–**f**) Conventional angiographic images acquired from early arterial phase to venous phase. (**a**, **b**) Signal voids in the high flow vessels can be depicted on both T1-weighted and T2-weighted MR images, including the feeding artery (*arrow*) and arterialized draining vein (*arrowhead*). (**c**) Coronal T2-weighted MR image reveals the nidus (*circle*). (**d**–**f**) Arteriogram acquired demonstrates a slightly enlarged tortuous artery (*arrow*) during the early arterial phase, the nidus (*star*) on late arterial phase, and then enlarged draining veins (*arrowheads*)

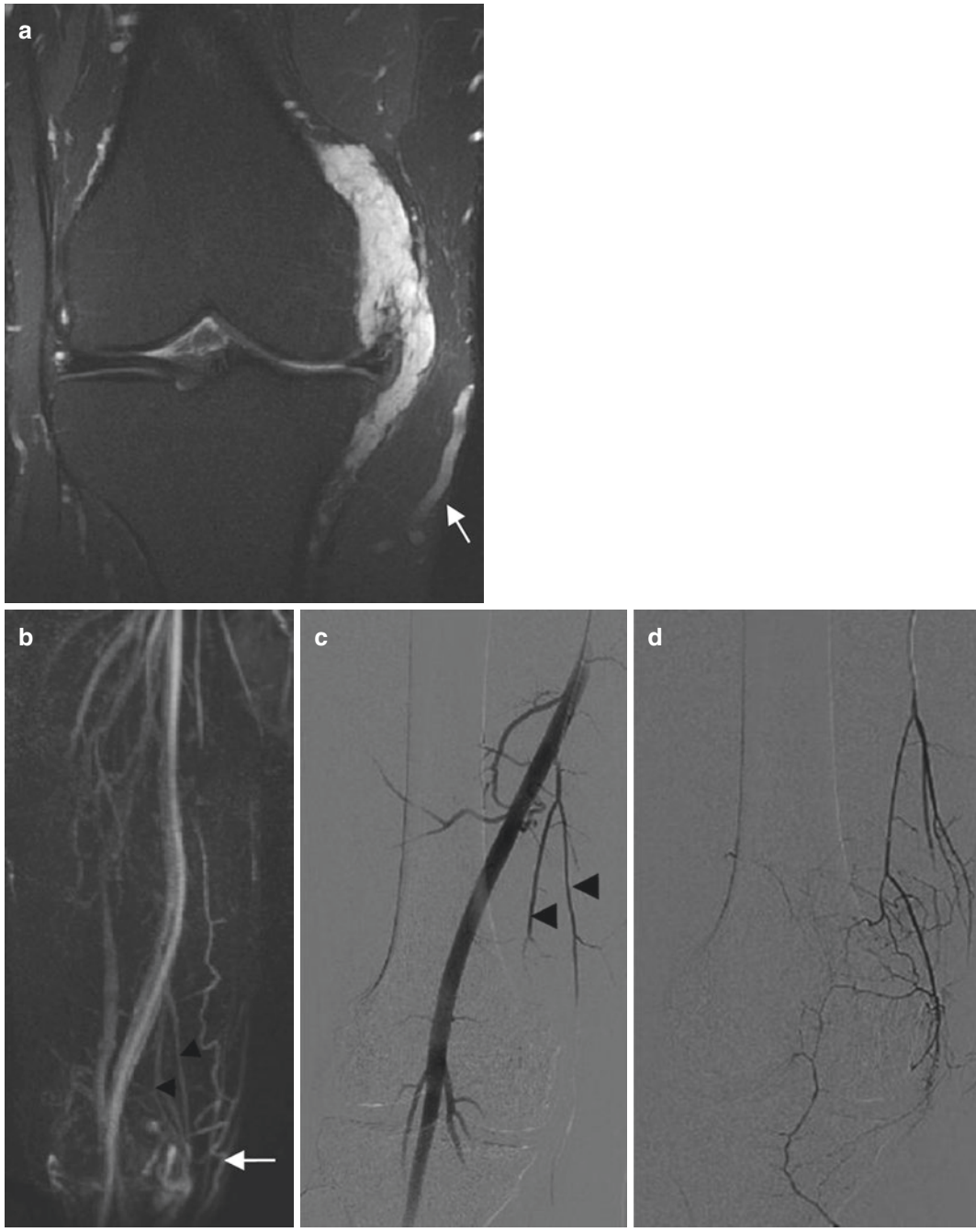

Fig. 16.18 Arteriovenous malformation of the knee in a 30-year-old man. (**a**) Coronal T2-weighted MR image with fat suppression. (**b**) Maximum intensity projection (MIP) after 3D contrast-enhanced MR angiography. (**c**, **d**) Conventional angiographic images acquired during early arterial phase before the treatment. (**a**) The lesion is composed of tortuous enlarged feeding arteries located within the medial collateral ligament with a distended vein. (**b**) Two feeding arteries (*black arrowheads*) are seen on MIP after 3D contrast-enhanced MR angiography, with the early venous feeding (*arrow*). (**c**, **d**) Conventional angiographic images confirm these findings and reveals the two feeding arteries (*arrowheads*) from the superficial femoral artery

The dynamic opacification, using time-resolved MR angiography, confirms the rapid flow when the period between the start and the maximal enhancement is 5–10 s [3, 52]. Intraosseous extension of the lesion can also be seen [68]. Arteriography is only performed when the MR features are equivocal or when embolization is considered. This technique has the advantage of selective catheterization of the feeding arteries with depiction of the nidus and early draining veins.

The goal of treatment for AVMs is the eradication of the nidus, causal factor of the shunt. Treatment includes two stages, a preoperative embolization by a biological glue and a complete surgical excision [57]. Different surgical approaches have been described, including arterial microcatheterism, direct percutaneous puncture, and retrograde venous microcatheterism [45].

Key Points

1. Arteriovenous malformations
2. Ill-defined area with multiple vessels (arteries with diastolic flow/arterialized draining veins with pulsatile flow)
3. Early venous filling

16.5 Particular Vascular Lesions

16.5.1 Glomus Tumor (GT)

According to the latest revision of the WHO classification (2013), glomus tumor is regarded as a pericystic (perivascular) tumor (see also Chaps. 11 and 15).

Glomus tumors and its rare variants, such as glomangioma (20 % of cases), glomangiomyoma (less than 10 % of cases), and the exceptional malignant glomus tumor [69], are derived from neuromyoarterial glomus bodies. These millimeter organs are involved in thermoregulation by modulation of cutaneous blood flow. They are mainly localized in the dermis, at the ends of fingers and toes, and especially under the nails [38, 70]. The most common location for GTs is the tip of the fingers, particularly the subungual area where it can lead to erosion of the adjacent phalanx [71]. They are less common in the pulp. They are mainly observed in adults and are observed as a small red-blue superficial nodule (1 mm−3 cm), with extremely intense focal pain, triggered by pressure and cold [70]. This clinical presentation results in diagnosis in 90 % of the cases when the digits are involved [72]. Subungual lesions have female predilection in contrast to the other locations [70, 73]. Other rare locations include muscles, tendons, nerves, bones, and viscera [74–76] and involve less specific symptoms [70].

On radiography, finger involvement is accompanied by bone erosion of the distal phalanx in approximately one-third of the cases [72]. GTs can be visualized using MRI or ultrasound, although they typically measures only 1.5–2 mm [77, 78]. Ultrasound shows a well-limited hypoechoic nodule which often contains small cystic internal rearrangements and a significant hyperemia on Doppler (Fig. 16.19) [79]. On MRI, dedicated coils and very thin sections with excellent spatial resolution should be used. GTs show with hypo- to iso-signal intensity on T1-weighted images and strong hypersignal intensity on T2-weighted images (Fig. 16.20) [28, 75]. MR angiography shows intense enhancement in the arterial phase with tumor blush [71, 78,

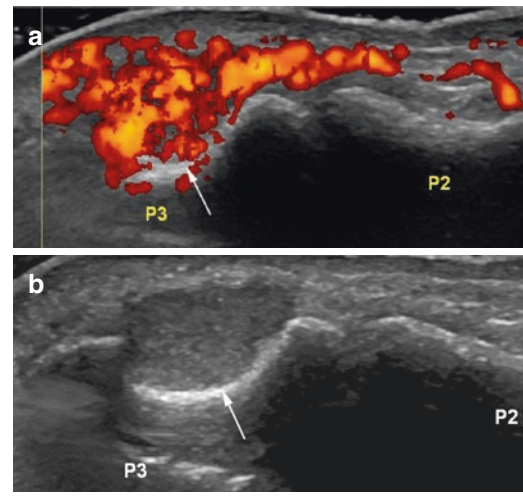

Fig. 16.19 Glomus tumor of the nail bed. (**a**) Ultrasound. (**b**) Power Doppler image. (**a**) Ultrasound images show an isoechogenic mass eroding the underlying distal phalanx (*P3*) (*arrow*). The lesion is markedly hypervascular (**b**) on power Doppler image

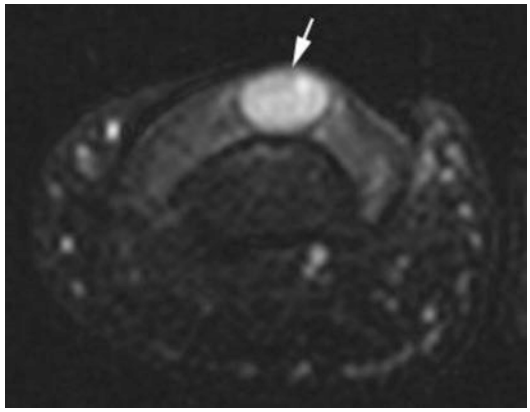

Fig. 16.20 Glomus tumor of the nail bed. Axial T2-weighted MR image with fat suppression shows a 2 mm markedly hyperintense lesion of the nail bed

80]. This is sometimes the sole sequence showing the lesion. Small lesions enhance homogeneously after gadolinium administration, while larger GTs are more heterogeneous on T2-weighted images and after contrast administration [79]. The histologic subtype of the lesion (vascular, solid, myxoid) also influences its appearance on T1-weighted images (from low to high signal intensity) [71]. Postsurgical recurrences present the typical appearance of GTs in half of the cases [78]. The main differential diagnoses include mucoid cysts, venous malformations, malignant melanomas, soft tissue chondromas, giant cell tumors, and epidermoid cysts [71, 75, 78, 80].

Surgical excision must be complete to be effective for pain and prevent recurrences (4–20 % in the subungual location) [77].

Key Points

1. Glomus tumor
2. Benign tumor of the neuromyoarterial glomus bodies
3. Tip of the fingers, mainly in the subungual area
4. Highly suggestive clinical presentation: small red-blue nodule, intense focal pain triggered by pressure and cold
5. Small highly vascular lesion of the nail bed, possible erosion of the adjacent bone

16.5.2 Synovial Hemangioma (SH)

SHs are rare vascular lesion of the synovial membrane that affect children and young adults, and 75 % of patients are symptomatic before the age of 16 years [81]. SHs mainly develop in the knee (60 %), particularly at the suprapatellar pouch. Other locations include the elbow (30 %), ankle, hip, temporomandibular joint, and tendon sheaths [81, 82]. SH may be associated with repetitive episodes of pain, swelling, and joint effusion (hemarthrosis). With time, limitation of the joint mobility and muscle atrophy can develop. Joint blocking is possible when the lesion is pedunculated. A diagnostic delay is common, and because of the repetitive bleeding into the joint, an arthropathy similar to the hemophilic arthropathy can develop. If arthrography is performed, the synovium may demonstrate irregular contours mimicking synovial chondromatosis, villonodular synovitis, or rheumatoid arthritis [82]. MRI is the best imaging modality to identify this lesion and to assess its intra- and extraarticular extent (Fig. 16.21). MRI features are usually pathognomonic: serpiginous lesion with a low or iso-signal intensity on T1-weighted images and high signal intensity on T2-weighted images due to vascular stasis, associated with fibrofatty septa and sometimes vascular structures (thrombosed or not). SH lesion enhances after gadolinium administration, sometimes heterogeneously. Joint effusion and erosive changes of the subchondral bone are often associated [83, 84].

Early surgical excision is mandatory to prevent the development of arthropathy.

16.6 Syndromes Associated with Vascular Lesions

Several well-known familial or sporadic syndromes include vascular tumors or malformations (Table 16.4) [67, 85, 86]. Most of them develop during childhood and require long-term therapeutic planning (based on the flow velocity) [67]. These patients must be followed by a multidisciplinary team.

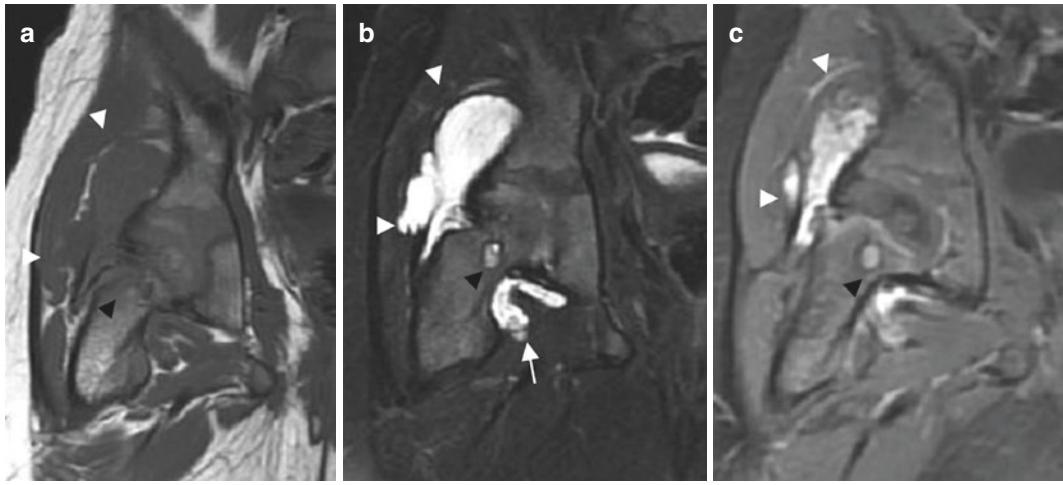

Fig. 16.21 Synovial hemangioma of the hip. (**a**) Coronal T1-weighted MR image. (**b**) Coronal T2-weighted MR image with fat suppression. (**c**) Coronal T1-weighted MR image after Gadolinium contrast administration with fat suppression. Hemangioma demonstrates a low signal intensity on T1-WI, bright signal intensity on T2-WI and enhances after gadolinium administration (*white arrowheads*). Note the hypointense area under the femoral head related to hemosiderin deposition (*arrow*) and the erosive change of the anterior aspect of the femoral neck (*black arrowhead*)

Table 16.4 Main syndromes associated with vascular tumors and malformations

Tumors		
PHACE syndrome/PELVIS and SACRAL syndrome: infantile hemangioma		
Kasabach-Merritt syndrome: kaposiform hemangioendotheliomas, tufted angiomas		
Malformations		
Syndrome	Hemodynamic	Main location
Klippel-Trenaunay	Low-flow	Extremities
Maffucci	Low-flow	Extremities
Parkes Weber	High-flow	Extremities
Sturge-Weber	Low-flow	Head
Proteus	Low-flow	Diffuse
Rendu-Osler-Weber	High-flow	Diffuse

16.6.1 PHACE Syndrome

PHACE is an acronym for the syndrome's most common clinical and imaging findings: posterior fossa malformations, segmental infantile hemangiomas of the face and neck (usually larger than 5 cm), arterial anomalies, cardiac defects or coarctation of the aorta, eye or endocrine anomalies, and sternal defects [67, 87].

16.6.2 PELVIS and SACRAL Syndromes

Infantile hemangiomas located in the lumbosacral and perineal region are at risk of underlying developmental anomalies, particularly spinal dysraphisms, anorectal and urinary tract defects. These associations have been variably named in the literature with several acronyms:

- *PELVIS* for Perineal hemangioma, External genitalia malformations, Lipomyelomeningocele, Vesicorenal abnormalities, Imperforate anus, and Skin tag
- *SACRAL* for Spinal dysraphism, Anogenital anomalies, Cutaneous malformations, Renal and urological anomalies, and Angioma of Lumbosacral localization

Evaluation with MRI is therefore recommended for such lesions in this particular location [88, 89].

16.6.3 Kasabach-Merritt Syndrome

Kasabach-Merritt syndrome is characterized by a combination of vascular lesions (kaposiform

hemangioendotheliomas, tufted angiomas), thrombocytopenia, and coagulopathy causing hemorrhage, infections, and multiple organ failure [67]. The mortality rate is close to 30 % [38], and aggressive therapy is required (steroids, vincristine, and interferons).

16.6.4 Klippel-Trenaunay Syndrome

Klippel-Trenaunay syndrome is a non-hereditary complex disorder usually affecting only one of the lower extremities, but it can spread into the pelvis and trunk. It is defined by three classic clinical findings: (1) capillary malformation (usually of affected limb), (2) bone and soft tissue limb enlargement (usually affecting one extremity), and (3) atypical varicosities or venous malformations with a characteristic abnormal lateral vein beginning at the ankle and extending to the pelvic region (Fig. 16.22) [67, 90].

Abnormal development of the deep and superficial veins explains persistent embryonic veins including lateral veins with persistent sciatic vein

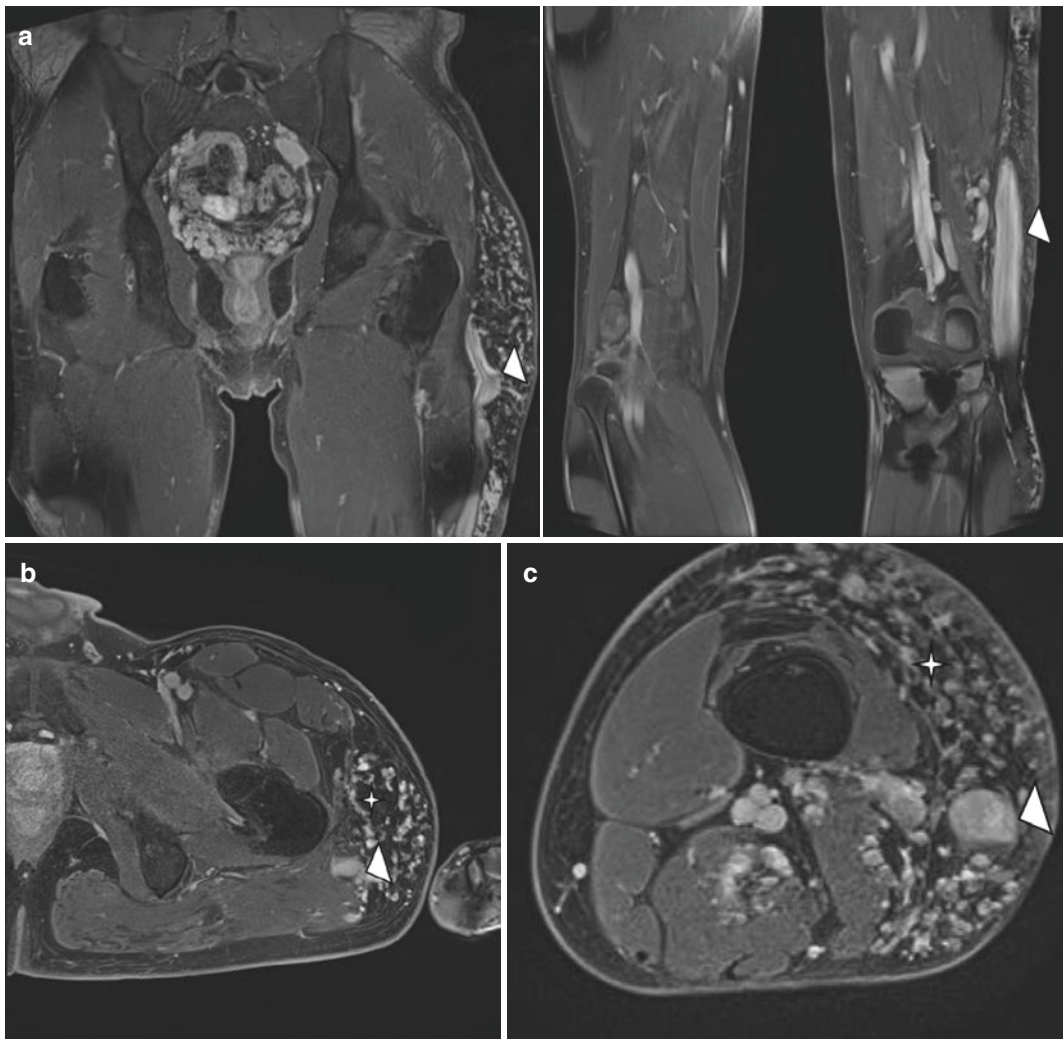

Fig. 16.22 Klippel-Trenaunay syndrome in a 30-year-old boy. (**a**) Coronal T2-weighted MR image with fat suppression. (**b**, **c**) Axial T2-weighted MR images with fat suppression of the pelvis and thigh. (**a–c**) There is hemihypertrophy of left lower extremity with extensive subcutaneous (*star*) and intramuscular venous malformations. Note the characteristic abnormal sapheneous vein (*arrowhead* in **c**)

and dilated superficial system. Hypertrophy is variable, affecting the whole leg or only the distal digits [91]. Syndactyly, polydactyly, and congenital hip dislocation can also be observed [92].

On imaging, vascular overgrowth demonstrates slow and late enhancement indicating low-flow malformations. Deep venous malformations of the femoral vein are commonly seen. Because of overgrowth of the soft tissues, the affected limb is usually larger and longer than the unaffected limb [86].

16.6.5 Maffucci Syndrome

Maffucci syndrome is a rare and non-hereditary syndrome characterized by the association of multiple enchondromas and multiple low-flow vascular malformations (mainly venous, rarely lymphatic) [93]. Clinically, it manifests before 1 year of age in 25 % of the patients and by the puberty in 80 % of all cases [67].

Enchondromas usually involve the phalanges of the hands (Fig. 16.23) and feet, and in one-half of the patients, lesions are unilateral and lead to the development of notable malformations [93]. Low-flow vascular malformations do not have the same distribution as enchondromas and usually involve the subcutaneous soft tissues of another anatomic region. Phleboliths are very suggestive [94].

The malignant transformation rate is high and involves enchondromas (chondrosarcoma) in 15–20 % of the patients [95] or vascular malformations (angiosarcoma) in 3–5 % of the cases [96]. There is also a higher incidence of other malignant tumors, such as gliomas and ovarian and pancreatic tumors. A long-term follow-up is therefore mandatory [93].

16.6.6 Parkes Weber Syndrome

Parkes Weber syndrome combines a cutaneous capillary malformation with limb hemihypertrophy, congenital varicose veins, and arteriovenous malformations (a major difference with Klippel-Trenaunay syndrome). Numerous small periarticular arteriovenous fistulas or shunts can be detected in the affected limb [97]. Cardiac failure occurs in some patients with high blood flow vascular malformations.

Fig. 16.23 Maffuci syndrome. Plain radiograph of the hand. Multiple, expansible, well-defined and predominantly lytic lesions within the phalanges and metacarpals of the hand (*stars*) correspond to multiple enchondromas. The presence of phleboliths (*arrows*) within the soft tissue are highly suggestive of a Maffuci syndrome

16.6.7 Rendu-Osler-Weber Syndrome

Hereditary hemorrhagic telangiectasia (Rendu-Osler-Weber syndrome) is a genetic, autosomal dominant disorder. It is characterized by telangiectasia and arteriovenous malformations in specific locations, leading to epistaxis and hemorrhage into the digestive tract [98]. Lesions commonly involve the mucous membranes, skin, lungs, and genitourinary and gastrointestinal systems. At imaging, Rendu-Osler-Weber syndrome is characterized by arteriovenous malformations or fistulas in the lungs, liver, central nervous system, or other sites [99].

Key Points

1. Different terminology for designating vascular tumors may cause confusion. The revised WHO classification (2013) differs from ISSVA classification for benign lesions, but there is an overall agreement for intermediate and malignant lesions.
2. Infantile hemangioma is the most common vascular tumor in infancy.
3. Venous malformation represents the most common peripheral vascular malformation, followed by lymphatic malformation.
4. A number of familial or sporadic syndromes may be associated with vascular tumors and malformations.
5. The presence of phleboliths in a soft tissue mass on plain radiographs strongly suggests a venous malformation.
6. Ultrasound coupled with color Doppler US is the imaging modality of choice for the initial assessment and characterization of a lesion of presumed vascular origin.
7. MRI has a major role in defining the lesion's extent and therapy planning. Conventional angiography has been largely replaced by dynamic magnetic resonance (MR) angiography for the classification of vascular anomalies. Arteriography is only performed when MR features are equivocal or when embolization is considered.

References

1. Restrepo R (2013) Multimodality imaging of vascular anomalies. Pediatr Radiol 43(Suppl 1):S141–S154. doi:10.1007/s00247-012-2584-y
2. Dubois J, Alison M (2010) Vascular anomalies: what a radiologist needs to know. Pediatr Radiol 40:895–905. doi:10.1007/s00247-010-1621-y
3. Flors L, Leiva-Salinas C, Maged IM, Norton PT, Matsumoto AH, Angle JF, Hugo Bonatti M, Park AW, Ahmad EA, Bozlar U, Housseini AM, Huerta TE, Hagspiel KD (2011) MR imaging of soft-tissue vascular malformations: diagnosis, classification, and therapy follow-up. Radiogr Rev Publ Radiol Soc N Am Inc 31:1321–1340. doi:10.1148/rg.315105213, -1341
4. Cohen MM (2007) Hemangiomas: their uses and abuses. Am J Med Genet A 143A:235–240. doi:10.1002/ajmg.a.31571
5. Fletcher C, Bridge J, World Health Organization (2013) Classification of tumours of soft tissue and bone. IRAC, Lyon
6. ISSVA Classification of Vascular Anomalies ©2014 International Society for the Study of Vascular Anomalies Available at "issva.org/classification"
7. Enzinger F, Weiss S (1995) Benign tumors and tumor-like lesions of blood vessels. In: Enzinger FM, Weiss SW (eds) Soft tissue tumors, 3rd edn. Mosby, St. Louis, pp 579–626
8. Mulliken JB, Glowacki J (1982) Hemangiomas and vascular malformations in infants and children: a classification based on endothelial characteristics. Plast Reconstr Surg 69:412–422
9. Enjolras O, Wassef M, Chapot R (2007) Color atlas of vascular tumors and vascular malformations. Cambridge University Press, Cambridge
10. Navarro OM, Laffan EE, Ngan B-Y (2009) Pediatric soft-tissue tumors and pseudo-tumors: MR imaging features with pathologic correlation: part 1. Imaging approach, pseudotumors, vascular lesions, and adipocytic tumors. Radiogr Rev Publ Radiol Soc N Am Inc 29:887–906. doi:10.1148/rg.293085168
11. Cohen MM (2006) Vascular update: morphogenesis, tumors, malformations, and molecular dimensions. Am J Med Genet A 140:2013–2038. doi:10.1002/ajmg.a.31333
12. Mulliken J (1993) Cutaneous vascular anomalies. Semin Vasc Surg 6(4):204–218
13. Mulliken J (2006) Mulliken and Young's vascular anomalies: hemangiomas and malformations, 1st edn. Oxford University Press, Oxford
14. Berenguer B, Mulliken JB, Enjolras O, Boon LM, Wassef M, Josset P, Burrows PE, Perez-Atayde AR, Kozakewich HPW (2003) Rapidly involuting congenital hemangioma: clinical and histopathologic features. Pediatr Dev Pathol Off J Soc Pediatr Pathol Paediatr Pathol Soc 6:495–510
15. Moukaddam H, Pollak J, Haims AH (2009) MRI characteristics and classification of peripheral vascular malformations and tumors. Skeletal Radiol 38:535–547. doi:10.1007/s00256-008-0609-2
16. Kwon E-KM, Seefeldt M, Drolet BA (2013) Infantile hemangiomas: an update. Am J Clin Dermatol 14:111–123. doi:10.1007/s40257-013-0008-x
17. Dubois J, Rypens F (2009) Vascular anomalies. Ultrasound Clin 4:471–495
18. North PE, Waner M, Mizeracki A, Mrak RE, Nicholas R, Kincannon J, Suen JY, Mihm MC (2001) A unique microvascular phenotype shared by juvenile hemangiomas and human placenta. Arch Dermatol 137:559–570

19. Finn MC, Glowacki J, Mulliken JB (1983) Congenital vascular lesions: clinical application of a new classification. J Pediatr Surg 18:894–900
20. Degrugillier-Chopinet C, Bisdorff-Bresson A, Laurian C, Breviere G-M, Staumont D, Fayoux P, Lenica D, Gautier C (2011) Role of duplex Doppler for superficial "angiomas". J Mal Vasc 36:348–354. doi:10.1016/j.jmv.2011.08.003
21. Konez O, Burrows PE (2002) Magnetic resonance of vascular anomalies. Magn Reson Imaging Clin N Am 10(363–388):vii
22. Metry DW, Dowd CF, Barkovich AJ, Frieden IJ (2001) The many faces of PHACE syndrome. J Pediatr 139:117–123. doi:10.1067/mpd.2001.114880
23. Léauté-Labrèze C, Taïeb A (2008) Efficacy of beta-blockers in infantile capillary haemangiomas: the physiopathological significance and therapeutic consequences. Ann Dermatol Venereol 135:860–862. doi:10.1016/j.annder.2008.10.006
24. Gorincour G, Kokta V, Rypens F, Garel L, Powell J, Dubois J (2005) Imaging characteristics of two subtypes of congenital hemangiomas: rapidly involuting congenital hemangiomas and non-involuting congenital hemangiomas. Pediatr Radiol 35:1178–1185. doi:10.1007/s00247-005-1557-9
25. Nasseri E, Piram M, McCuaig CC, Kokta V, Dubois J, Powell J (2014) Partially involuting congenital hemangiomas: a report of 8 cases and review of the literature. J Am Acad Dermatol 70:75–79. doi:10.1016/j.jaad.2013.09.018
26. Lowe LH, Marchant TC, Rivard DC, Scherbel AJ (2012) Vascular malformations: classification and terminology the radiologist needs to know. Semin Roentgenol 47:106–117. doi:10.1053/j.ro.2011.11.002
27. Enjolras O, Soupre V, Picard A (2004) Anomalies vasculaires superficielles (« angiomes »). EMC Pédiatrie 2004:98-745-A-10
28. Kransdorf M, Murphey M (2006) Imaging of soft tissue tumors, 2nd edn. WB Saunders Company, Philadelphia
29. Park S-W, Kim H-J, Sung KJ, Lee JH, Park IS (2012) Kimura disease: CT and MR imaging findings. AJNR Am J Neuroradiol 33:784–788. doi:10.3174/ajnr.A2854
30. Lalaji TA, Haller JO, Burgess RJ (2001) A case of head and neck kaposiform hemangioendothelioma simulating a malignancy on imaging. Pediatr Radiol 31:876–878. doi:10.1007/s002470100009
31. Hermans DJJ, van Beynum IM, van der Vijver RJ, Kool LJS, de Blaauw I, van der Vleuten CJM (2011) Kaposiform hemangioendothelioma with Kasabach-Merritt syndrome: a new indication for propranolol treatment. J Pediatr Hematol Oncol 33:e171–e173. doi:10.1097/MPH.0b013e3182152e4e
32. Fahrtash F, McCahon E, Arbuckle S (2010) Successful treatment of kaposiform hemangioendothelioma and tufted angioma with vincristine. J Pediatr Hematol Oncol 32:506–510. doi:10.1097/MPH.0b013e3181e001a9
33. Restrepo CS, Ocazionez D (2011) Kaposi's sarcoma: imaging overview. Semin Ultrasound CT MR 32:456–469. doi:10.1053/j.sult.2011.03.007
34. Weiss SW, Enzinger FM (1982) Epithelioid hemangioendothelioma: a vascular tumor often mistaken for a carcinoma. Cancer 50:970–981
35. Bruegel M, Waldt S, Weirich G, Woertler K, Rummeny EJ (2006) Multifocal epithelioid hemangioendothelioma of the phalanges of the hand. Skeletal Radiol 35:787–792. doi:10.1007/s00256-005-0943-6
36. Nuthakki S, Fessell D, Lal N, Shirkhoda A, Irwin T, Irwin R (2007) Epithelioid hemangioendothelioma mimicking a nerve sheath tumor clinically and on MR imaging. Skeletal Radiol 36(Suppl 1):S58–S62. doi:10.1007/s00256-006-0197-y
37. El Demellawy D, Nasr A, Alowami S (2009) Epithelioid hemangioendothelioma of the temporal artery presenting as temporal arteritis: case report and literature review. Rare Tumors 1:e20. doi:10.4081/rt.2009.e20
38. Weiss S, Goldblum J, Enzinger F (2008) Enzinger and Weiss's soft tissue tumors. Mosby Elsevier, Philadelphia
39. Meis-Kindblom JM, Kindblom LG (1998) Angiosarcoma of soft tissue: a study of 80 cases. Am J Surg Pathol 22:683–697
40. Nakazono T, Kudo S, Matsuo Y, Matsubayashi R, Ehara S, Narisawa H, Yonemitsu N (2000) Angiosarcoma associated with chronic lymphedema (Stewart-Treves syndrome) of the leg: MR imaging. Skeletal Radiol 29:413–416
41. Rossi S, Fletcher CDM (2002) Angiosarcoma arising in hemangioma/vascular malformation: report of four cases and review of the literature. Am J Surg Pathol 26:1319–1329
42. Jackson IT, Carreño R, Potparic Z, Hussain K (1993) Hemangiomas, vascular malformations, and lymphovenous malformations: classification and methods of treatment. Plast Reconstr Surg 91:1216–1230
43. Dubois J, Soulez G, Oliva VL, Berthiaume MJ, Lapierre C, Therasse E (2001) Soft-tissue venous malformations in adult patients: imaging and therapeutic issues. Radiogr Rev Publ Radiol Soc N Am Inc 21:1519–1531. doi:10.1148/radiographics.21.6.g01nv031519
44. Fayad LM, Fayad L, Hazirolan T, Bluemke D, Mitchell S (2006) Vascular malformations in the extremities: emphasis on MR imaging features that guide treatment options. Skeletal Radiol 35:127–137. doi:10.1007/s00256-005-0057-1
45. Cahill AM, Nijs ELF (2011) Pediatric vascular malformations: pathophysiology, diagnosis, and the role of interventional radiology. Cardiovasc Intervent Radiol 34:691–704. doi:10.1007/s00270-011-0123-0
46. Bruder E, Alaggio R, Kozakewich HPW, Jundt G, Dehner LP, Coffin CM (2012) Vascular and perivascular lesions of skin and soft tissues in children and adolescents. Pediatr Dev Pathol Off J Soc Pediatr Pathol Paediatr Pathol Soc 15:26–61. doi:10.2350/11-11-1119-PB.1

47. Dompmartin A, Ballieux F, Thibon P, Lequerrec A, Hermans C, Clapuyt P, Barrellier M-T, Hammer F, Labbé D, Vikkula M, Boon LM (2009) Elevated D-dimer level in the differential diagnosis of venous malformations. Arch Dermatol 145:1239–1244. doi:10.1001/archdermatol.2009.296
48. Wassef M (2011) Vascular tumors and pseudotumors: introduction. Ann Pathol 31:410–412. doi:10.1016/j.annpat.2011.05.013
49. Goto T, Kojima T, Iijima T, Yokokura S, Kawano H, Yamamoto A, Matsuda K (2001) Soft-tissue haemangioma and periosteal new bone formation on the neighbouring bone. Arch Orthop Trauma Surg 121:549–553
50. Sung MS, Kang HS, Lee HG (1998) Regional bone changes in deep soft tissue hemangiomas: radiographic and MR features. Skeletal Radiol 27:205–210
51. Herborn CU, Goyen M, Lauenstein TC, Debatin JF, Ruehm SG, Kröger K (2003) Comprehensive time-resolved MRI of peripheral vascular malformations. AJR Am J Roentgenol 181:729–735. doi:10.2214/ajr.181.3.1810729
52. Ohgiya Y, Hashimoto T, Gokan T, Watanabe S, Kuroda M, Hirose M, Matsui S, Nobusawa H, Kitanosono T, Munechika H (2005) Dynamic MRI for distinguishing high-flow from low-flow peripheral vascular malformations. AJR Am J Roentgenol 185:1131–1137. doi:10.2214/AJR.04.1508
53. Buetow PC, Kransdorf MJ, Moser RP, Jelinek JS, Berrey BH (1990) Radiologic appearance of intramuscular hemangioma with emphasis on MR imaging. AJR Am J Roentgenol 154:563–567. doi:10.2214/ajr.154.3.2154914
54. Redondo P, Aguado L, Martínez-Cuesta A (2011) Diagnosis and management of extensive vascular malformations of the lower limb: Part I. Clinical diagnosis. J Am Acad Dermatol 65:893–906. doi:10.1016/j.jaad.2010.12.047
55. Enjolras O, Ciabrini D, Mazoyer E, Laurian C, Herbreteau D (1997) Extensive pure venous malformations in the upper or lower limb: a review of 27 cases. J Am Acad Dermatol 36:219–225
56. Dompmartin A, Vikkula M, Boon LM (2010) Venous malformation: update on aetiopathogenesis, diagnosis and management. Phlebol Venous Forum R Soc Med 25:224–235. doi:10.1258/phleb.2009.009041
57. Brevière G, Degrugillier-Chopinet C, Bisdorff-Bresson A (2011) Anomalies vasculaires superficielle. EMC Cardiologie 6:1–21
58. Sidhu MK, Perkins JA, Shaw DWW, Bittles MA, Andrews RT (2005) Ultrasound-guided endovenous diode laser in the treatment of congenital venous malformations: preliminary experience. J Vasc Interv Radiol 16:879–884. doi:10.1097/01.RVI.0000163005.50283.62
59. Marler JJ, Mulliken JB (2005) Current management of hemangiomas and vascular malformations. Clin Plast Surg 32(99–116):ix. doi:10.1016/j.cps.2004.10.001
60. Cahill AM, Nijs E, Ballah D, Rabinowitz D, Thompson L, Rintoul N, Hedrick H, Jacobs I, Low D (2011) Percutaneous sclerotherapy in neonatal and infant head and neck lymphatic malformations: a single center experience. J Pediatr Surg 46:2083–2095. doi:10.1016/j.jpedsurg.2011.07.004
61. Chen EY, Hostikka SL, Oliaei S, Duke W, Schwartz SM, Perkins JA (2009) Similar histologic features and immunohistochemical staining in microcystic and macrocystic lymphatic malformations. Lymphat Res Biol 7:75–80. doi:10.1089/lrb.2009.0003
62. Blei F (2008) Congenital lymphatic malformations. Ann N Y Acad Sci 1131:185–194. doi:10.1196/annals.1413.016
63. Jeltsch M, Tammela T, Alitalo K, Wilting J (2003) Genesis and pathogenesis of lymphatic vessels. Cell Tissue Res 314:69–84. doi:10.1007/s00441-003-0777-2
64. Hogeling M, Adams S, Law J, Wargon O (2011) Lymphatic malformations: clinical course and management in 64 cases. Australas J Dermatol 52:186–190. doi:10.1111/j.1440-0960.2011.00777.x
65. Koeller KK, Alamo L, Adair CF, Smirniotopoulos JG (1999) Congenital cystic masses of the neck: radiologic-pathologic correlation. Radiogr Rev Publ Radiol Soc N Am Inc 19:121–146. doi:10.1148/radiographics.19.1.g99ja06121, -153
66. Zadvinskis DP, Benson MT, Kerr HH, Mancuso AA, Cacciarelli AA, Madrazo BL, Mafee MF, Dalen K (1992) Congenital malformations of the cervicothoracic lymphatic system: embryology and pathogenesis. Radiogr Rev Publ Radiol Soc N Am Inc 12:1175–1189. doi:10.1148/radiographics.12.6.1439020
67. Nozaki T, Nosaka S, Miyazaki O, Makidono A, Yamamoto A, Niwa T, Tsutsumi Y, Aida N, Masaki H, Saida Y (2013) Syndromes associated with vascular tumors and malformations: a pictorial review. Radiogr Rev Publ Radiol Soc N Am Inc 33:175–195. doi:10.1148/rg.331125052
68. Ernemann U, Kramer U, Miller S, Bisdas S, Rebmann H, Breuninger H, Zwick C, Hoffmann J (2010) Current concepts in the classification, diagnosis and treatment of vascular anomalies. Eur J Radiol 75:2–11. doi:10.1016/j.ejrad.2010.04.009
69. Kayal JD, Hampton RW, Sheehan DJ, Washington CV (2001) Malignant glomus tumor: a case report and review of the literature. Dermatol Surg Off Publ Am Soc Dermatol Surg Al 27:837–840
70. Schiefer TK, Parker WL, Anakwenze OA, Amadio PC, Inwards CY, Spinner RJ (2006) Extradigital glomus tumors: a 20-year experience. Mayo Clin Proc 81:1337–1344. doi:10.4065/81.10.1337
71. Drapé JL, Idy-Peretti I, Goettmann S, Wolfram-Gabel R, Dion E, Grossin M, Benacerraf R, Guérin-Surville H, Bittoun J (1995) Subungual glomus tumors: evaluation with MR imaging. Radiology 195:507–515. doi:10.1148/radiology.195.2.7724775
72. Van Geertruyden J, Lorea P, Goldschmidt D, de Fontaine S, Schuind F, Kinnen L, Ledoux P, Moermans JP (1996) Glomus tumours of the hand. A retrospective study of 51 cases. J Hand Surg Br Edinb Scotl 21:257–260

73. Lee D-W, Yang J-H, Chang S, Won C-H, Lee M-W, Choi J-H, Moon K-C (2011) Clinical and pathological characteristics of extradigital and digital glomus tumours: a retrospective comparative study. J Eur Acad Dermatol Venereol 25:1392–1397. doi:10.1111/j.1468-3083.2011.03979.x
74. Lee S, Le H, Munk P, Malfair D, Lee CH, Clarkson P (2010) Glomus tumour in the forearm: a case report and review of MRI findings. JBR-BTR 93:292–295
75. Baek HJ, Lee SJ, Cho KH, Choo HJ, Lee SM, Lee YH, Suh KJ, Moon TY, Cha JG, Yi JH, Kim MH, Jung S-J, Choi JH (2010) Subungual tumors: clinicopathologic correlation with US and MR imaging findings. Radiogr Rev Publ Radiol Soc N Am Inc 30:1621–1636. doi:10.1148/rg.306105514
76. González-Llanos F, López-Barea F, Isla A, Fernández-Prieto A, Zubillaga A, Alvarez F (2000) Periosteal glomus tumor of the femur: a case report. Clin Orthop 380:199–203
77. Netscher DT, Aburto J, Koepplinger M (2012) Subungual glomus tumor. J Hand Surg 37:821–823. doi:10.1016/j.jhsa.2011.10.026; quiz 824
78. Theumann NH, Goettmann S, Le Viet D, Resnick D, Chung CB, Bittoun J, Chevrot A, Drapé J-L (2002) Recurrent glomus tumors of fingertips: MR imaging evaluation. Radiology 223:143–151. doi:10.1148/radiol.2231010977
79. Glazebrook KN, Laundre BJ, Schiefer TK, Inwards CY (2011) Imaging features of glomus tumors. Skeletal Radiol 40:855–862. doi:10.1007/s00256-010-1067-1
80. Van Ruyssevelt CEA, Vranckx P (2004) Subungual glomus tumor: emphasis on MR angiography. AJR Am J Roentgenol 182:263–264. doi:10.2214/ajr.182.1.1820263
81. Devaney K, Vinh TN, Sweet DE (1993) Synovial hemangioma: a report of 20 cases with differential diagnostic considerations. Hum Pathol 24:737–745
82. Greenspan A, Azouz EM, Matthews J, Décarie JC (1995) Synovial hemangioma: imaging features in eight histologically proven cases, review of the literature, and differential diagnosis. Skeletal Radiol 24:583–590
83. Llauger J, Monill JM, Palmer J, Clotet M (1995) Synovial hemangioma of the knee: MRI findings in two cases. Skeletal Radiol 24:579–581
84. Narváez JA, Narváez J, Aguilera C, De Lama E, Portabella F (2001) MR imaging of synovial tumors and tumor-like lesions. Eur Radiol 11:2549–2560. doi:10.1007/s003300000759
85. Garzon MC, Huang JT, Enjolras O, Frieden IJ (2007) Vascular malformations. Part II: associated syndromes. J Am Acad Dermatol 56:541–564. doi:10.1016/j.jaad.2006.05.066
86. Elsayes KM, Menias CO, Dillman JR, Platt JF, Willatt JM, Heiken JP (2008) Vascular malformation and hemangiomatosis syndromes: spectrum of imaging manifestations. AJR Am J Roentgenol 190:1291–1299. doi:10.2214/AJR.07.2779
87. Oza VS, Wang E, Berenstein A, Waner M, Lefton D, Wells J, Blei F (2008) PHACES association: a neuroradiologic review of 17 patients. AJNR Am J Neuroradiol 29:807–813. doi:10.3174/ajnr.A0937
88. Drolet BA, Chamlin SL, Garzon MC, Adams D, Baselga E, Haggstrom AN, Holland KE, Horii KA, Juern A, Lucky AW, Mancini AJ, McCuaig C, Metry DW, Morel KD, Newell BD, Nopper AJ, Powell J, Frieden IJ (2010) Prospective study of spinal anomalies in children with infantile hemangiomas of the lumbosacral skin. J Pediatr 157:789–794. doi:10.1016/j.jpeds.2010.07.054
89. Stockman A, Boralevi F, Taïeb A, Léauté-Labrèze C (2007) SACRAL syndrome: spinal dysraphism, anogenital, cutaneous, renal and urologic anomalies, associated with an angioma of lumbosacral localization. Dermatol Basel Switz 214:40–45. doi:10.1159/000096911
90. Jacob AG, Driscoll DJ, Shaughnessy WJ, Stanson AW, Clay RP, Gloviczki P (1998) Klippel-Trénaunay syndrome: spectrum and management. Mayo Clin Proc 73:28–36. doi:10.1016/S0025-6196(11)63615-X
91. McGrory BJ, Amadio PC, Dobyns JH, Stickler GB, Unni KK (1991) Anomalies of the fingers and toes associated with Klippel-Trenaunay syndrome. J Bone Joint Surg Am 73:1537–1546
92. Kanterman RY, Witt PD, Hsieh PS, Picus D (1996) Klippel-Trenaunay syndrome: imaging findings and percutaneous intervention. AJR Am J Roentgenol 167:989–995. doi:10.2214/ajr.167.4.8819399
93. Zwenneke Flach H, Ginai AZ, Wolter Oosterhuis J (2001) Best cases from the AFIP. Maffucci syndrome: radiologic and pathologic findings. Armed Forces Institutes of Pathology. Radiogr Rev Publ Radiol Soc N Am Inc 21:1311–1316. doi:10.1148/radiographics.21.5.g01se301311
94. Unger EC, Kessler HB, Kowalyshyn MJ, Lackman RD, Morea GT (1988) MR imaging of Maffucci syndrome. AJR Am J Roentgenol 150:351–353. doi:10.2214/ajr.150.2.351
95. Schwartz HS, Zimmerman NB, Simon MA, Wroble RR, Millar EA, Bonfiglio M (1987) The malignant potential of enchondromatosis. J Bone Joint Surg Am 69:269–274
96. Bach AD, Walgenbach KJ, Horch RE (2000) Hemangiosarcoma of the left hand in a patient with the rare combination of Maffucci's and Stewart Treves syndrome. Vasa 29:71–73. doi:10.1024/0301-1526.29.1.71
97. Ziyeh S, Spreer J, Rössler J, Strecker R, Hochmuth A, Schumacher M, Klisch J (2004) Parkes Weber or Klippel-Trenaunay syndrome? Non-invasive diagnosis with MR projection angiography. Eur Radiol 14:2025–2029. doi:10.1007/s00330-004-2274-8
98. McDonald J, Bayrak-Toydemir P, Pyeritz RE (2011) Hereditary hemorrhagic telangiectasia: an overview of diagnosis, management, and pathogenesis. Genet Med Off J Am Coll Med Genet 13:607–616. doi:10.1097/GIM.0b013e3182136d32
99. Jaskolka J, Wu L, Chan RP, Faughnan ME (2004) Imaging of hereditary hemorrhagic telangiectasia. AJR Am J Roentgenol 183:307–314. doi:10.2214/ajr.183.2.1830307